Molecular Pharmacology Fast Forward. Published on August 3, 2012 as doi:10.1124/mol.112.080531
This article has not been copyedited and formatted. The final version may differ from this version.

MOL #80531

Title: Investigating mGlu5 allosteric modulator cooperativity, affinity and agonism: enriching structure-function studies and structure-activity relationships

Karen J. Gregory, Meredith J. Noetzel, Jerri M. Rook, Paige N. Vinson, Shaun R. Stauffer, Alice L. Rodriguez, Kyle A. Emmitte, Ya Zhou, Aspen C. Chun, Andrew S. Felts, Brian A. Chauder, Craig W. Lindsley, Colleen M. Niswender and P. Jeffrey Conn

Vanderbilt Center for Neuroscience Drug Discovery, Vanderbilt University Medical Center, Nashville, TN, USA (K.J.G., M.J.N., J.M.R., P.N.V., S.R.S., A.L.R., K.A.E., Y.Z., A.C.C., A.S.F., B.A.C., C.W.L., C.M.N., P.J.C.)

Department of Pharmacology, Vanderbilt University Medical Center, Nashville, TN, USA (K.J.G., M.J.N., J.M.R., P.N.V., S.R.S., A.L.R., K.A.E., Y.Z., A.C.C., A.S.F., B.A.C., C.W.L., C.M.N., P.J.C.)

Drug Discovery Biology, Monash Institute of Pharmaceutical Sciences, Monash University, Parkville, VIC, Australia (K.J.G)

Department of Chemistry, Vanderbilt University Medical Center, Nashville, TN, USA (K.A.E., C.W.L.)

Molecular Pharmacology Fast Forward. Published on August 3, 2012 as DOI: 10.1124/mol.112.080531
This article has not been copyedited and formatted. The final version may differ from this version.

MOL #80531

Running title: Delineating mGlu5 modulator affinity and cooperativity

Corresponding Author:

P. Jeffrey Conn

1215 Light Hall

2215-B Garland Ave

Nashville, TN, USA

37232

Jeff.conn@vanderbilt.edu

Number of text pages: 30

Number of tables: 6

Number of figures: 9

Number of references: 59

Number of words in Abstract: 242

Number of words in Introduction: 674

Number of words in Discussion: 1499

Non-standard abbreviations:

[^{3}H]methoxyPEPy: [^{3}H]-3-methoxy-5-(pyridin-2-ylethynyl)pyridine; ADX47273: S-(4-fluoro-phenyl)-{3-[3-(4-fluoro-phenyl)-[1,2,4]oxadiazol-5-yl]-piperidin-1-yl}-methanone; ANOVA: analysis of variance; CDPPB: 3-cyano-N-(1,3-diphenyl-1H-pyrazol-5-yl)benzamide; CPPHA: N-{4-Chloro-2-[(1,3-dioxo-1,3-dihydro-2H-isoindol-

Molecular Pharmacology Fast Forward. Published on August 3, 2012 as DOI: 10.1124/mol.112.080531
This article has not been copyedited and formatted. The final version may differ from this version.

2-yl)methyl]phenyl}-2-hydroxybenzamide; DFB: difluorobenzaldazine; DMEM: Dulbecco's modified eagle medium; ERK1/2: extracellular signal-regulated kinases 1 and 2; FBS: fetal bovine serum; GPCR: G protein-coupled receptor; HEK: Human embryonic kidney; L-DOPA: L-3,4-dihydroxyphenylalanine; M-5MPEP: 2-(2-(3-methoxyphenyl)ethynyl)-5-methylpyridine; mGlu: metabotropic glutamate receptor; MPEP: 2-methyl-6-(phenylethynyl)-pyridine; MTEP: 3-[(2-methyl-1,3-thiazol-4-yl)ethynyl]pyridine; NAM: negative allosteric modulator; PAM: positive allosteric modulator; pERK1/2: phosphorylated extracellular signal-regulated kinases 1 and 2; PET: positron emission tomography; SAM: silent allosteric modulator; SAR: structure-activity relationship; SIB-1757: 6-methyl-2-(phenylazo)-3-pyridinol; SIB-1893: (E)-2-methyl-6-(2-phenylethenyl)-pyridine; VU0092273: 1-{[4-(2-phenylethynyl)phenyl]carbonyl}piperidin-4-ol; VU0285683: 3-fluoro-5-[3-(pyridin-2-yl)-1,2,4-oxadiazol-5-yl]benzonitrile; VU0357121: 4-butoxy-N-(2,4-difluorophenyl)benzamide; VU0360172: N-cyclobutyl-6-((3-fluorophenyl)ethynyl)nicotinamide hydrochloride; VU0364289: 2-{4-[2-(benzyloxy)acetyl]piperazin-1-yl}benzonitrile; VU0366248: N-(3-chloro-2-fluorophenyl)-3-cyano-5-fluorobenzamide; VU0366249: N-(3-chloro-4-fluorophenyl)-3-cyano-5-fluorobenzamide; VU0405386: N-(tert-butyl)-5-((3-fluorophenyl)ethynyl)picolinamide; VU0405398: (5-((3-fluorophenyl)ethynyl)pyridin-2-yl)(3-hydroxyazetidin-1-yl)methanone; VU0415051: N-tert-butyl-6-[2-(3-fluorophenyl)ethynyl]pyridine-3-carboxamide; VU0366058: 2-(1,3-benzoxazol-2-ylamino)-4-(4-fluorophenyl)pyrimidine-5-carbonitrile; VU29: 4-nitro-N-(1,3-diphenyl-1H-pyrazol-5-yl)benzamide;

Molecular Pharmacology Fast Forward. Published on August 3, 2012 as DOI: 10.1124/mol.112.080531
This article has not been copyedited and formatted. The final version may differ from this version.

Abstract

Increasingly, drug discovery programs are focusing on allosteric modulators as a means to modify activity of G protein-coupled receptor (GPCR) targets. Allosteric binding sites are topographically distinct from the endogenous ligand-(orthosteric) binding site, allowing for co-occupation of a single receptor with the endogenous ligand and an allosteric modulator that can alter receptor pharmacology. Negative allosteric modulators (NAMs) inhibit, while positive allosteric modulators (PAMs) enhance, the affinity and/or efficacy of the orthosteric agonist. Established approaches for estimating affinities and efficacy of orthosteric ligands are not appropriate for allosteric modulators and this raises challenges in fully understanding the actions of novel modulators of GPCRs. Metabotropic glutamate receptor 5 ($mGlu_5$) is a family C GPCR for which a large array of allosteric modulators has been identified. We have taken advantage of the wealth of tools for probing allosteric sites on $mGlu_5$ to validate an operational model of allosterism that allows quantitative estimates of modulator affinity and cooperativity. Affinity estimates derived from functional assays fit well with measured affinities from radioligand binding experiments for both PAMs and NAMs from diverse chemical scaffolds with varying degrees of cooperativity. Interestingly, we observed modulation bias for PAMs when comparing $mGlu_5$-mediated Ca^{++} mobilization and phosphorylation of ERK1/2. Furthermore, we utilize this model to quantify the impact of mutations that reduce binding or potentiation by PAMs. This model can be applied to PAM and NAM potency curves in combination with maximal fold shift data to derive reliable estimates of modulator affinity.

Molecular Pharmacology Fast Forward. Published on August 3, 2012 as DOI: 10.1124/mol.112.080531
This article has not been copyedited and formatted. The final version may differ from this version.

Introduction

The metabotropic glutamate receptors (mGlus) are G protein-coupled receptors for the neurotransmitter glutamate that play important roles in regulating a range of major circuits in the central nervous system. The mGlus include eight subtypes, $mGlu_1$- $mGlu_8$ (Niswender and Conn, 2010). Historically, it has been difficult to develop ligands with high subtype selectivity among the mGlus due to the high sequence conservation of the orthosteric (i.e., glutamate) binding site. This has led to the search for compounds that interact with these receptors at "allosteric" sites that are topographically distinct from the orthosteric glutamate binding site. These compounds, referred to as allosteric modulators, can affect the affinity and/or efficacy of an orthosteric ligand, a property referred to as cooperativity, allowing them to modulate endogenous agonist activity. Modulators that inhibit orthosteric ligand binding and/or activity are negative allosteric modulators (NAMs) while those that enhance are positive allosteric modulators (PAMs); a third category, silent (or neutral) allosteric modulators (SAMs), includes compounds that bind but do not modulate the response to orthosteric agonist.

Allosteric modulators offer a number of theoretical advantages over their competitive counterparts in addition to improvements in receptor selectivity (Melancon et al., 2012). For modulators that possess no intrinsic efficacy, there is the potential for spatial and temporal modulation of receptor activity. This is an especially important consideration for potential CNS therapeutics, where 'fine-tuning' neurotransmission is likely to yield a better therapeutic outcome than the sustained blockade of or activation by an orthosteric ligand. Furthermore, the cooperativity between the two sites is

Molecular Pharmacology Fast Forward. Published on August 3, 2012 as DOI: 10.1124/mol.112.080531
This article has not been copyedited and formatted. The final version may differ from this version.

saturable, such that allosteric modulators have a built-in "ceiling level" to their effect, and may therefore have a larger therapeutic index.

Efforts to develop allosteric modulators of one mGlu subtype, $mGlu_{5,}$ have been especially successful and a broad range of allosteric modulators as well as radioligands for allosteric sites have been developed for this mGlu subtype. Since the first identification of SIB-1757 (6-methyl-2-(phenylazo)-3-pyridinol) and SIB-1893 ((E)-2-methyl-6-(2-phenylethenyl)-pyridine), and structural analogues MPEP (2-methyl-6-(phenylethynyl)-pyridine) and MTEP (3-[(2-methyl-1,3-thiazol-4-yl)ethynyl]pyridine), as selective $mGlu_5$ NAMs (Varney et al., 1999; Gasparini et al., 1999; Cosford et al., 2003a), a diverse array of allosteric modulators have now been identified, including pure PAMs, PAMs with agonist activity, weak and full NAMs and SAMs (O'Brien et al., 2004; Kinney et al., 2005; Rodriguez et al., 2005, 2009, 2010; Chen et al., 2007, 2008; Liu et al., 2008; Noetzel et al., 2012). $mGlu_5$ PAMs have potential utility for treatment of cognitive disorders and schizophrenia, whereas NAMs are being pursued for treatment of Fragile X Syndrome, depression, anxiety, L-DOPA-induced dyskinesia and gastroesophogeal reflux disorder (Niswender and Conn, 2010).

In allosteric modulator drug discovery programs, potency and maximal effect are routinely used to drive iterative medicinal chemistry efforts and select compounds for further characterization. Commonly, NAMs are assessed for inhibition of a sub-maximal (EC_{80}) concentration of orthosteric agonist, while PAMs are assayed for potentiation of a low agonist concentration (EC_{20}) (Melancon et al., 2012). However, PAM or NAM potencies represent the combined contribution of modulator affinity and cooperativity with agonist and are also dependent upon the agonist concentration present (Gregory et

Molecular Pharmacology Fast Forward. Published on August 3, 2012 as DOI: 10.1124/mol.112.080531
This article has not been copyedited and formatted. The final version may differ from this version.

al., 2010). Furthermore, allosteric modulator structure-activity relationships (SAR) are often 'steep', and small changes in a molecule can result in complete loss of activity, which could be related to changes in modulator cooperativity and/or affinity (Wood et al., 2011). Finally, allosteric ligands are prone to 'molecular switches', where subtle changes to a NAM scaffold yields a PAM or vice versa, an effect relating to cooperativity changes (Wood et al., 2011). Thus, validated approaches for quantitative analysis of allosteric modulator pharmacology are needed to delineate cooperativity versus affinity. We have taken advantage of the large range of tools to study allosteric sites on $mGlu_5$ to validate the use of the operational model of allosterism (Leach et al., 2007). Our data suggest that this quantitative model provides a robust method to delineate cooperativity and affinity from modulator potency curves. Derivation of affinity estimates from functional assays will be especially useful in assessing affinities of novel allosteric modulators that act at sites for which radioligands have yet to be developed.

Molecular Pharmacology Fast Forward. Published on August 3, 2012 as DOI: 10.1124/mol.112.080531
This article has not been copyedited and formatted. The final version may differ from this version.

Materials and Methods

Materials

Dulbecco's Modified Eagle's Medium (DMEM), fetal bovine serum (FBS) and antibiotics were purchased from Invitrogen (Carlsbad, CA). [^{3}H]methoxyPEPy (76.3 Ci/mmol) was custom synthesized by PerkinElmer Life and Analytical Sciences (Waltham, MA). CDPPB (3-cyano-N-(1,3-diphenyl-1H-pyrazol-5-yl)benzamide), VU29 (4-nitro-N-(1,3-diphenyl-1H-pyrazol-5-yl)benzamide), CPPHA (N-{4-Chloro-2-[(1,3-dioxo-1,3-dihydro-2H-isoindol-2-yl)methyl]phenyl}-2-hydroxybenzamide), VU0357121 (4-butoxy-N-(2,4-difluorophenyl)benzamide), VU0364289 (2-{4-[2-(benzyloxy)acetyl]piperazin-1-yl}benzonitrile), VU0092273 (1-{[4-(2-phenylethynyl)phenyl]carbonyl}piperidin-4-ol), VU0360172 (N-cyclobutyl-6-((3-fluorophenyl)ethynyl)nicotinamide hydrochloride), VU0285683 (3-fluoro-5-[3-(pyridin-2-yl)-1,2,4-oxadiazol-5-yl]benzonitrile), VU0366058 (2-(1,3-benzoxazol-2-ylamino)-4-(4-fluorophenyl)pyrimidine-5-carbonitrile), M-5MPEP (2-(2-(3-methoxyphenyl)ethynyl)-5-methylpyridine), VU0366248 (N-(3-chloro-2-fluorophenyl)-3-cyano-5-fluorobenzamide) and VU0366249 (N-(3-chloro-4-fluorophenyl)-3-cyano-5-fluorobenzamide) were all synthesized in-house using previously reported methodologies (Kinney et al., 2005; Chen et al., 2007, 2008; Felts et al., 2010; Hammond et al., 2010; Zhou et al., 2010; Rodriguez et al., 2005 & 2010; Mueller et al., 2012). VU0405398 ((5-((3-fluorophenyl)ethynyl)pyridin-2-yl)(3-hydroxyazetidin-1-yl)methanone), VU0405386 (N-(tert-butyl)-5-((3-fluorophenyl)ethynyl)picolinamide) and VU0415051 (N-tert-butyl-6-[2-(3-fluorophenyl)ethynyl]pyridine-3-carboxamide) were synthesized in-house utilizing the methods described in supplementary materials. Unless otherwise stated, all

Molecular Pharmacology Fast Forward. Published on August 3, 2012 as DOI: 10.1124/mol.112.080531
This article has not been copyedited and formatted. The final version may differ from this version.

other reagents were purchased from Sigma-Aldrich (St. Louis, MO) and were of an analytical grade.

Cell culture and mutagenesis

Mutations were introduced into the wild type rat $mGlu_5$ in pCI:Neo using site-directed mutagenesis (Quikchange II, Agilent, Santa Clara, CA) and verified by sequencing. Wild type and mutant rat $mGlu_5$ receptor constructs were transfected into HEK293A cells, using Fugene6^{TM} (Promega, Madison, WI) as the transfection reagent. Polyclonal stable cell lines were derived for rat $mGlu_5$ mutant constructs by maintaining the cells at sub-confluence for a minimum of four passages in the presence of 1 mg/ml G418 (Mediatech, Manassas, VA). Stably transfected cell lines were subsequently maintained in complete DMEM supplemented with 10% fetal bovine serum (FBS), 2 mM L-glutamine, 20 mM HEPES, 0.1 mM Non-Essential Amino Acids, 1 mM sodium pyruvate, antibiotic-antimycotic and 500 μg/ml G418 at 37°C in a humidified incubator containing 5% CO_2, 95% O_2.

Intracellular Ca^{2+} mobilization

The day prior to assay, HEK293A-rat $mGlu_5$ cells were seeded at 50,000 cells/well in poly-D-lysine coated black-walled, clear bottom 96 well plates in assay medium (DMEM supplemented with 10% dialyzed fetal bovine serum, 20 mM HEPES and 1 mM sodium pyruvate). On the day of assay, the cell permeant Ca^{2+} indicator dye Fluo-4 (Invitrogen, Carlsbad, CA) was used to assay receptor-mediated Ca^{2+} mobilization as described previously (Hammond et al., 2010) using a Flexstation II (Molecular

Molecular Pharmacology Fast Forward. Published on August 3, 2012 as DOI: 10.1124/mol.112.080531
This article has not been copyedited and formatted. The final version may differ from this version.

Devices, Sunnyvale, CA). A 5-point smoothing function was applied to the raw fluorescent Ca^{2+} traces and basal fluorescence of individual wells determined during the first 20 sec. The peak increase in fluorescence over basal was determined prior to normalization to the maximal peak response elicited by glutamate.

ERK1/2 phosphorylation

Receptor-mediated extracellular signal-regulated kinases 1 and 2 (ERK1/2) phosphorylation was determined using the AlphaScreen™-based ERK SureFire™ kit (PerkinElmer Life and Analytical Sciences, Boston, MA & TGR Biosciences, Thebarton, Australia). HEK293A-rat-$mGlu_5$ cells were plated at a density of 40,000 cells/well in clear 96 well poly-D-lysine coated plates in assay medium 16-24 hr prior to assay. Media was aspirated and cells washed once with serum-free media (DMEM supplemented with 16 mM HEPES) then serum starved for a minimum of 6 hr prior to assay. Serum-free media was exchanged for fresh 20 min prior to exposure to modulators and/or glutamate. At room temperature, the time course for $mGlu_5$ mediated ERK phosphorylation was characterized by an initial peak at 7-8 min that returned to baseline levels by 15 min (data not shown). Subsequently, for interaction experiments with allosteric modulators, cells were exposed to allosteric modulator or vehicle 1 min prior to stimulation with glutamate for 7 min. Assay was terminated by aspiration of ligand containing media and addition of 50 µl/well of Lysis buffer. Following agitation for 10 min, 4 µl of lysate was transferred to a white 384-well plate (Costar, Corning Life Sciences, Tewksbury, MA). Under light diminished conditions, 7 µl/well of Reaction buffer mixture (containing 1 part Activation buffer to 6 parts Reaction buffer and 1:250 (v/v) donor and acceptor beads) was added.

Molecular Pharmacology Fast Forward. Published on August 3, 2012 as DOI: 10.1124/mol.112.080531
This article has not been copyedited and formatted. The final version may differ from this version.

After 90 min incubation at 37°C, AlphaScreen signal was measured using a H4 synergy reader (Biotek, Winooski, VT) with standard AlphaScreen settings. Data are expressed as fold increase over basal levels of phosphorylated ERK.

Radioligand binding

Membranes were prepared from HEK293A cells expressing rat $mGlu_5$ and mutants thereof as follows. Cells were harvested by trypsinization and pelleted by centrifugation for 3 min at 300 x*g*. Cell pellets were re-suspended in ice-cold homogenization buffer (50 mM Tris-HCl, 10 mM EDTA, 0.9% NaCl, pH7.4), and homogenized by 3 x 10 sec bursts with a Tekmar TP-18/10S1 homogenizer (Tekmar, Cincinnati, OH) separated by 30 sec on ice. Cell fractions were separated by centrifugation at 1000 x*g* for 10 min. Supernatant was then centrifuged for 1 hr at 30,000 x*g* and the resulting pellet re-suspended in ice-cold Ca^{2+} assay buffer. For saturation binding experiments, membranes (20-50 µg/well) were incubated with a range of [^{3}H]-3-methoxy-5-(pyridin-2-ylethynyl)pyridine ([^{3}H]methoxyPEPy) concentrations (0.5 nM-60 nM) for 1 hr at room temperature with shaking in Binding Buffer (50 mM Tris-HCl, 0.9% NaCl, pH7.4). 10 µM MPEP was used to determine non-specific binding. For inhibition binding experiments, membranes were incubated with ~2 nM [^{3}H]methoxyPEPy and a range of concentrations of test ligand (100 pM-100 µM) in the absence or presence of 1 mM glutamate (added simultaneously) for 1 hr at room temperature with shaking in Ca^{2+} assay buffer with 1% DMSO final. Binding assays were terminated by rapid filtration through GF/B Unifilter plates (PerkinElmer Life and Analytical Sciences, Boston, MA) using a Brandel 96-well plate Harvester (Brandel Inc.,

Molecular Pharmacology Fast Forward. Published on August 3, 2012 as DOI: 10.1124/mol.112.080531
This article has not been copyedited and formatted. The final version may differ from this version.

Gaithersburg, MD), and three washes with ice-cold Binding Buffer, separating bound from free radioligand. Plates were allowed to dry overnight prior to addition of MicroScint 20 (40 µl/well; PerkinElmer). Radioactivity was counted after at least 2 hr incubation using a TopCount Scintillation Counter (PerkinElmer Life and Analytical Sciences, Boston, MA).

Data Analysis

All computerized nonlinear regression was performed using Prism 5.01 (GraphPad Software, San Diego, CA).

Inhibition [^{3}H]methoxyPEPy binding data sets were fitted to a one-site inhibition binding model and estimates of inhibitor dissociation constants (K_I) were derived using the Cheng-Prusoff equation for competitive ligands (Cheng and Prusoff, 1973). For ligands that did not fully displace radioligand, the following version of the allosteric ternary complex model (Lazareno and Birdsall, 1995) was fitted to inhibition binding data:

$$\frac{Y}{Y_{max}} = \frac{[D]}{[D] + \frac{K_D\left(1+\frac{[B]}{K_B}\right)}{\left(1+\frac{\alpha[B]}{K_B}\right)}} \qquad \text{(equation 1)}$$

where Y/Y_{max} is the fractional specific binding, D is the radioligand concentration, B is the molar concentration of the allosteric modulator, K_D is the radioligand equilibrium dissociation constant, K_B is the allosteric modulator equilibrium dissociation constant. α denotes the cooperativity factor, where values of $\alpha > 1$ describe positive cooperativity, values of $\alpha < 1$ (but greater the 0) denote negative cooperativity and $\alpha = 1$ denotes neutral cooperativity.

Molecular Pharmacology Fast Forward. Published on August 3, 2012 as DOI: 10.1124/mol.112.080531
This article has not been copyedited and formatted. The final version may differ from this version.

Shifts of glutamate concentration-response curves by allosteric modulators were globally fitted to an operational model of allosterism (Leach et al., 2007):

$$Effect = \frac{E_m(\tau_A[A](K_B+\alpha\beta[B])+\tau_B[B]K_A)^n}{([A]K_B+K_AK_B+K_A[B]+\alpha[A][B])^n+(\tau_A[A](K_B+\alpha\beta[B])+\tau_B[B]K_A)^n} \quad \text{(equation 2)}$$

where A is the molar concentration of orthosteric agonist glutamate, K_A is the equilibrium dissociation constant of the orthosteric agonist, glutamate, and K_B and B are as described above. Affinity modulation is governed by the cooperativity factor α, and efficacy modulation is governed by β. The parameters τ_A and τ_B relate to the ability of the orthosteric and allosteric ligands, respectively, to engender receptor activation. E_m and *n* denote the maximal possible system response and the transducer function that links occupancy to response, respectively. Unless otherwise stated all parameters were derived from global fitting glutamate concentration-response curves in the absence and presence of allosteric modulators.

In the absence of discernible allosteric agonism it was assumed $\tau_B = 0$, such that equation 2 simplifies to:

$$Effect = \frac{E_m(\tau_A[A](K_B+\alpha\beta[B]))^n}{([A]K_B+K_AK_B+K_A[B]+\alpha[A][B])^n+(\tau_A[A](K_B+\alpha\beta[B])^n} \quad \text{(equation 3)}$$

Theoretical PAM or NAM concentration-response curves in the presence of different concentrations of agonist were derived from progressive fold-shifts of an agonist concentration response curve simulated using equation 3. For these simulations the following parameters were held constant for both NAMs and PAMs: $pK_A = 6$, $pK_B = 7$, $\tau_A = 10$, $\log\alpha = 0$, $n = 2$, $E_m = 100$, basal = 0. Modulator concentrations spanned 100 pM-30 μM; cooperativity for PAMs was set to $\log\beta = 1$, while for NAMs, β was assumed to approach zero, such that $\log\beta = -100$.

Molecular Pharmacology Fast Forward. Published on August 3, 2012 as DOI: 10.1124/mol.112.080531
This article has not been copyedited and formatted. The final version may differ from this version.

An alternative, simplified, version of this operational model was applied to estimate a composite cooperativity parameter (αβ) for PAMs (Leach et al., 2007):

$$y = basal + \frac{(E_m - basal)(\tau_A[A](K_B + \alpha\beta[B]) + \tau_B[B]K_A)^n}{(\tau_A[A](K_B + \alpha\beta[B]) + \tau_B[B]K_A)^n + (K_A(K_B + [B]))^n} \quad \text{(equation 4)}$$

where basal denotes the baseline level (ligand-independent) of the system response and all other parameters are as described above for equation 2.

Allosteric modulator and agonist concentration-response curves were fitted to a four parameter logistic equation in order to determine potency estimates:

$$y = \frac{bottom + (top - bottom)}{(1 + 10^{(logEC_{50} - A)HillSlope}} \quad \text{(equation 5)}$$

where *bottom* and *top* are the lower and upper plateaus, respectively, of the concentration-response curve, HillSlope is the Hill coefficient that describes the steepness of the curve, A is the molar concentration of orthosteric agonist glutamate and EC_{50} is the molar concentration of modulator required to generate a response halfway between the *top* and *bottom.*

Allosteric modulator concentration-response curves were also fitted to the following version of the operational model of allosterism (equation 7) in concert with a control glutamate concentration-response curve (equation 6) to estimate modulator affinity and cooperativity.

Control:

$$y = basal + \frac{E_m - basal}{1 + \frac{K_A + [A]}{\tau_A + [A]}} \quad \text{(equation 6)}$$

Modulator:

$$y = basal + \frac{(E_m - basal)(\tau_A[A](K_B + \alpha\beta[B]))^n}{(\tau_A[A](K_B + \alpha\beta[B])^n + ([A]K_B + K_A K_B + K_A[B] + \alpha[A][B])^n} \quad \text{(equation 7)}$$

Molecular Pharmacology Fast Forward. Published on August 3, 2012 as DOI: 10.1124/mol.112.080531
This article has not been copyedited and formatted. The final version may differ from this version.

where all parameters are as described above for equations 2 and 3. K_A, τ_A, E_m and basal were shared across analyses; for modulator curves, A was held constant to the molar agonist concentration, either EC_{20} for PAMs or EC_{80} for NAMs, present in the assay.

All affinity, cooperativity and potency parameters were estimated as logarithms and are expressed as the mean ± S.E.M. Statistical analyses were performed where appropriate as indicated using: one-way ANOVA with Dunnett's post test when comparing to control, or Tukey's post-test when making multiple comparisons.

Molecular Pharmacology Fast Forward. Published on August 3, 2012 as DOI: 10.1124/mol.112.080531
This article has not been copyedited and formatted. The final version may differ from this version.

Results

Allosteric modulators are routinely screened for their potencies at either inhibiting the response to a submaximal concentration of orthosteric agonist or potentiating the response to a low concentration of agonist. However, allosteric modulator potency is dependent upon the concentration of orthosteric agonist utilized (Figure 1A, 1B). Analysis of the available literature for $mGlu_5$ NAMs (Figure 1C) reveals that potencies and affinities are well correlated and potencies for the majority of $mGlu_5$ NAMs lie within 10 fold of their affinity estimates. In contrast, the potencies of $mGlu_5$ PAMs are often higher than their estimated affinities at the prototypical allosteric site labeled by [^{3}H]MPEP and [^{3}H]methoxyPEPy (dePaulis et al., 2006; Liu et al., 2008; Vanejevs et al., 2008; Rodriguez et al., 2010; Sams et al., 2011; Zou et al., 2011). Only 15 reported $mGlu_5$ PAMs (out of 61) have potency values that lie within 10 fold of their affinity estimates (Figure 1D). These discrepancies are likely due to the influence of cooperativity with glutamate, since modulator potency reflects the combined contribution of modulator affinity and cooperativity. Also, some of these investigated PAMs do not bind in a completely competitive manner with the labeled site so that affinity estimates based on equations assuming competitive interactions from equilibrium competition binding analysis may not reflect actual affinities (Chen et al., 2008; Hammond et al., 2010). The vast majority of NAMs that have been investigated are structurally related to the NAM radioligands ([^{3}H]MPEP and [^{3}H]methoxyPEPy) used to measure affinity whereas the PAMs belong to a broader range of structural classes.

Given the discrepancies in measures of potencies versus affinity estimates, we were interested in using $mGlu_5$ as a model system to validate utilization of the operational

Molecular Pharmacology Fast Forward. Published on August 3, 2012 as DOI: 10.1124/mol.112.080531
This article has not been copyedited and formatted. The final version may differ from this version.

model of allosterism originally developed by Leach et al. (2007) to quantify allosteric interactions. In this model, K_A is the equilibrium dissociation constant of the orthosteric agonist and K_B the equilibrium dissociation constant of allosteric modulator. The coupling efficiencies of the orthosteric agonist and an allosteric modulator are described by τ_A and τ_B respectively. Modulation of affinity when the receptor is simultaneously bound is represented by the cooperativity factor, α, while efficacy modulation is governed by a second cooperativity factor, β.

Estimation of allosteric modulator affinity for $mGlu_5$ using radioligand binding assays

A total of 16 $mGlu_5$ allosteric modulators were chosen for validation of affinity and cooperativity estimates (Figure 2). These compounds represent 11 different chemical scaffolds and a diverse spectrum of allosteric modulator activities including pure PAMs, PAMs with agonist activity, full NAMs and weak NAMs (also referred to as partial antagonists, or NAMs with low negative cooperativity) (Gasparini et al., 1999; Kinney et al., 2005; Chen et al., 2007, 2008; Felts et al., 2010; Hammond et al., 2010; Zhou et al., 2010; Rodriguez et al., 2005, 2010; Mueller et al., 2012). Inhibition of [^{3}H]methoxyPEPy binding to HEK293A cell membranes stably expressing rat $mGlu_5$ (HEK293A-$mGlu_5$-wt) showed that affinity estimates for these allosteric modulators spanned greater than three orders of magnitude (Figure 3; Table 1). A number of modulators did not fully displace [^{3}H]methoxyPEPy binding. VU0357121 was previously reported to not significantly displace [^{3}H]methoxyPEPy binding (Hammond et al., 2010). However, we employed a different cell background and assay conditions (low $mGlu_5$ expression, 1% DMSO, Ca^{2+} assay buffer compared with high $mGlu_5$ expression and a Tris-based buffer) and observed

Molecular Pharmacology Fast Forward. Published on August 3, 2012 as DOI: 10.1124/mol.112.080531
This article has not been copyedited and formatted. The final version may differ from this version.

~35% displacement at 30 μM. This is consistent with an allosteric interaction between [^{3}H]methoxyPEPy and VU0357121. As such, the inhibition curve for VU0357121 was fitted to the allosteric ternary complex model (equation 1) to estimate affinity and cooperativity between these two allosteric sites. Similarly CPPHA, VU29 and VU0360172 were also fitted to this model. In the case of VU0364289 and VU0366249, inhibition was consistent with competitive binding limited by solubility. Inhibition binding for a representative compound from each chemical scaffold was also assessed in the presence of a saturating concentration of glutamate (1mM); consistent with previous reports (Cosford et al., 2003b; Bradley et al., 2011), glutamate had no effect on [^{3}H]methoxyPEPy specific binding. The presence of glutamate had no effect on the apparent affinity of these modulators, nor the cooperativity (logα) between the apparently non-competitive PAMs and [^{3}H]methoxyPEPy (Table 1).

Estimation of allosteric modulator affinity for $mGlu_5$ using receptor-mediated Ca^{2+} mobilization assay

Shifts in the glutamate concentration-response curves for intracellular Ca^{2+} mobilization was assessed for all 16 modulators (supplementary data figure 1; Noetzel et al., 2012) and a representative pure PAM, CPPHA (Figure 4A), a PAM with agonist activity, CDPPB (Figure 4B), a full NAM, MPEP (Figure 4C) and two weak NAMs, M-5MPEP and VU0366249 (Figure 4D, E) are shown. To derive estimates of allosteric modulator affinity and cooperativity, data sets were globally fitted to an operational model of allosterism (equation 2) where the affinity of glutamate (pK_A) was held constant, based on the value generated from a previous report, where glutamate affinity

Molecular Pharmacology Fast Forward. Published on August 3, 2012 as DOI: 10.1124/mol.112.080531
This article has not been copyedited and formatted. The final version may differ from this version.

was determined using the orthosteric radioligand, [^{3}H]quisqualate (Mutel et al., 2000). With respect to analysis of interactions between glutamate and PAMs, a composite cooperativity parameter (logαβ) that incorporates both affinity and efficacy modulation was first derived (Table 2). However, in order to allow for changes in the maximal response to glutamate, an effect driven by β, it was necessary to consider these two aspects of cooperativity independently. Constraining α to be neutral between glutamate and each of the PAMs yielded similar estimates of PAM affinity (pK_B) compared with determining affinity based on composite cooperativity logαβ (Table 2; Figure 4F). The interaction between glutamate and PAMs at $mGlu_5$ in this assay, therefore, can be solely accommodated by efficacy cooperativity (logβ; Figure 4G). With respect to NAMs, a composite cooperativity parameter, logαβ, could not be derived since changes in agonist E_{max} are an effect mediated solely by β. Instead, α was either derived alongside β or constrained to equal 1; NAMs showed either neutral α cooperativity or low positive α values (Table 3). The assumption that α=1 yielded similar estimates of pK_B for all NAMs and log β values for weak NAMs (Figure 4F; 4G). Strong correlation was observed between modulator affinity estimates derived from these functional interaction assays compared with pK_I values from inhibition of [^{3}H]methoxyPEPy binding experiments (Figure 4H). In general, the functional estimate of modulator affinity was within 3 fold of that derived from binding data. Similarly, in a high $mGlu_5$ expressing cell line, allosteric modulator affinity estimates for both PAMs and NAMs showed good agreement with those from the low expressing line (Figure 5F).

Molecular Pharmacology Fast Forward. Published on August 3, 2012 as DOI: 10.1124/mol.112.080531
This article has not been copyedited and formatted. The final version may differ from this version.

Quantifying allosteric modulator agonist activity and cooperativity with glutamate using receptor-mediated intracellular Ca^{2+} mobilization

High $mGlu_5$ expression in HEK293 cells results in a greater propensity for the exhibition of agonist activity by PAMs (Noetzel et al., 2012). The high expressing $mGlu_5$ HEK293 cell line has a 3 fold higher density of $mGlu_5$ than the low expressing cell line (2.3 ± 0.04 pmol/mg versus 0.6 ± 0.1 pmol/mg; data not shown). Interestingly, glutamate potency was lower in the high expressing cell line compared with the low expressing cells (541 ± 0.31 nM versus 149 ± 0.08 nM), corresponding to a 2.4 fold decrease in glutamate coupling efficiency ($\log\tau_A$; 0.37 ± 0.02 versus 0.80 ± 0.02). Within the operational model of allosterism, the capacity for intrinsic activity by an allosteric modulator is described by $\log\tau_B$. Phenotypic differences in modulator pharmacology were observed between the high and low expressing $mGlu_5$ HEK293A cell lines (Figure 4A-E and Figure 5A-E). With the exception of VU0357121, all PAMs showed an increase in agonist activity or $\log\tau_B$ (Table 2). Cooperativity ($\log\beta$) of PAMs was similar when comparing the low and high expressing cell lines, with the exception of VU0405386 and VU0405398, for which cooperativity was significantly increased by 3 fold (VU0405386: 0.54 ± 0.07 vs 1.10 ± 0.16, VU0405398: 0.30 ± 0.04 vs 0.87 ± 0.06, in low and high expressing cell lines respectively). For the three modulators classified as weak NAMs in the low-expressing cell line (M-5MPEP, VU0366248 and VU0366249), phenotypic changes in pharmacology were observed, with greater depressions in the glutamate E_{max} observed in the high expressing cell line (Figure 5D,E, supplementary figure 2). VU0366249 decreased the E_{max} of glutamate by ~40% in the high-expressing cell line compared with ~15% in the low-expressing line; however, the $\log\beta$ was similar in both

Molecular Pharmacology Fast Forward. Published on August 3, 2012 as DOI: 10.1124/mol.112.080531
This article has not been copyedited and formatted. The final version may differ from this version.

cell lines. M-5MPEP and VU0366248 fully abolished the response to glutamate in the high expressing cell line. Complete abrogation of the glutamate E_{max} may be indicative of increased negative cooperativity for these two modulators such that $\beta = 0$; however, with the low coupling efficiency of glutamate in the high-expressing cell line, NAMs with $\beta < 0.1$ are indistinguishable from $\beta = 0$. Given this potential for phenotypic differences in allosteric modulator pharmacology, a second measure of receptor function was employed to examine compound activity.

Quantifying allosteric modulator pharmacology using $mGlu_5$-mediated phosphorylation of extracellular signal-regulated kinases 1 and 2

Allosteric modulator pharmacology in our low-expressing HEK293A-$mGlu_5$ cell line most closely resembles observed pharmacology in astrocytes (Noetzel et al., 2012). Therefore, translocation of the glutamate-mediated ERK1/2 phosphorylation (pERK1/2) concentration response curve was assessed in the presence of each of the 16 allosteric modulators (Figures 6A-E, supplementary data figure 3) in the low-expressing cell line alone. Glutamate had ~10 fold lower coupling efficiency for pERK1/2, as evidence by its decreased potency (149 ± 0.08 nM versus 8671 ± 5071 nM) and $\log t_A$ (0.80 ± 0.02 versus -0.36 ± 0.13) relative to that for Ca^{2+} mobilization in the same cell line. Modulator affinity estimates from these pERK1/2 assays showed significant correlation with those derived from Ca^{2+} mobilization assays in the same cell background (Figure 6F). Overall, log beta values for all PAMs were lower for pERK1/2 compared with Ca^{2+} assay data. However, each of the PAMs showed intrinsic activity for pERK1/2 (Figure 6A,B; Table 4). VU0357121, VU0415051 and VU0405398, compounds that showed weaker

Molecular Pharmacology Fast Forward. Published on August 3, 2012 as DOI: 10.1124/mol.112.080531
This article has not been copyedited and formatted. The final version may differ from this version.

cooperativity in the Ca^{2+} mobilization assay, generally had lower $\log\tau_B$ values, while the remaining PAMs that showed more robust potentiation and/or agonist activity had higher $\log\tau_B$ values. With respect to NAMs, there was no evidence for inverse agonist activity; MPEP, VU0285683, VU0366058 and VU0366249 exhibited the same pharmacological profile as in the Ca^{2+} mobilization assay (Table 4; Figure 6C-E, supplementary figure 3). M-5MPEP (Figure 6E) and VU0366248 (supplementary figure 3) fully abolished pERK1/2 in response to glutamate, which may be indicative of higher negative cooperativity or reflect the decreased efficacy of glutamate in this assay.

Quantifying impact of single point mutations on allosteric modulator affinity and cooperativity

In addition to quantification of the affinity of different modulators across various assays, we were also interested in utilizing the model to quantify the impact of mutations on allosteric modulator pharmacology. Val substitution of Y658 and A809 has previously been described to result in a loss of appreciable [^{3}H]MPEP binding as well as potency for inhibition of quisqualate activity by MPEP (Pagano et al., 2000; Malherbe et al., 2003, 2006; Muhlemann et al., 2006). However, quantification of the effect on affinity and/or cooperativity has not been described. MPEP affinity was assessed from inhibition of glutamate concentration response curves for Ca^{2+} mobilization using stable polyclonal HEK293A cell lines expressing Y658V and A809V mutations of $mGlu_5$ (Figure 7). The pK_B of MPEP was reduced ~100 fold at A809V and Y658V compared to the estimate determined in the polyclonal HEK293A-$mGlu_5$-wild type cell line (Table 5). In addition, L743V is known to reduce the affinity of [^{3}H]MPEP by ~3 fold (Malherbe et al., 2003).

Molecular Pharmacology Fast Forward. Published on August 3, 2012 as DOI: 10.1124/mol.112.080531
This article has not been copyedited and formatted. The final version may differ from this version.

Herein, using a functional assay, MPEP pK_B was reduced 3 fold. At all three mutations, MPEP retained very high negative cooperativity with glutamate and was able to fully abolish the response. A809V has also been described to reduce potentiation by VU29 (Chen et al., 2008); analysis of glutamate potentiation by VU29 at this construct (Figure 8) showed significantly reduced affinity (30 fold; Table 5) compared to wild type. Cooperativity between glutamate and VU29 was unaffected by this mutation. Interestingly, L743V had no effect on the affinity of VU29 but did increase its cooperativity with glutamate (~3 fold). The non-MPEP site PAM, CPPHA, was previously reported to show a loss of potentiation at the F585I mutation at a single concentration (1μM; Chen et al., 2008). Compared to wild type, the affinity of CPPHA at the F585I construct was reduced ~3 fold; however, this did not reach significance (Figure 8; Table 5).

Estimating allosteric modulator affinity from modulator concentration response curves in the presence of a single concentration of agonist

The majority of drug discovery programs utilize concentration response curves for allosteric modulators in the presence of a single concentration of agonist (a low dose for potentiators, or a submaximal dose for inhibitors) in order to drive SAR. Therefore, we were interested in investigating whether or not valid estimates of affinity and/or cooperativity could be derived from such data sets. Simulations of the interaction between an agonist and PAM (Figure 1B) show that the PAM concentration response curve will translocate to the left in the presence of increasing concentrations of agonist. Conversely, for a NAM the concentration response curve will translocate to the right

Molecular Pharmacology Fast Forward. Published on August 3, 2012 as DOI: 10.1124/mol.112.080531
This article has not been copyedited and formatted. The final version may differ from this version.

(Figure 1A). For an allosteric modulator that potentiates to a level less than the maximal response to agonist or does not fully inhibit the response to agonist, modulator cooperativity and affinity can be determined directly from the modulator potency curve when assessed in parallel with the agonist concentration response curve (Figure 9A-C; Table 6). However, with a PAM (CPPHA or VU0364289) that potentiates the response to agonist to a level equal to/or greater than the maximal response to agonist alone, cooperativity and affinity cannot be extrapolated from such potency curves, since similar/identical potency and E_{max} estimates can be achieved with vastly different cooperativities/affinities. This is a consequence of the fact that the top plateau of the modulator concentration-response curve could reflect either achievement of the maximal system response or the limit of positive cooperativity. In order to determine CPPHA and VU0364289 pK_B estimates from potency curves, β was constrained such that the apparent cooperativity between these PAMs and glutamate were equal to the maximal leftward shift of the glutamate concentration response curve in the presence of a high concentration of potentiator (30 μM). Specifically, the log of the fold-shift caused by 30 μM VU0364289 (0.86 ± 0.06) and CPPHA (0.76 ± 0.13) was used to constrain logβ. Conversely, for NAMs that fully inhibited the response to glutamate, the cooperativity factor β was assumed to approach 0 (Figure 9C; Table 6). Using this approach, affinity estimates from modulator potency curves showed good correlation with those from more rigorous and time-consuming progressive fold shift analysis (Figure 9D). Cooperativity factors for weaker PAMs and NAMs from potency analysis agreed well with those determined from progressive fold shift analysis (Figure 9E; Table 6).

Molecular Pharmacology Fast Forward. Published on August 3, 2012 as DOI: 10.1124/mol.112.080531
This article has not been copyedited and formatted. The final version may differ from this version.

Discussion

Drug discovery programs for GPCRs are heavily reliant upon functional assays for primary screening, lead identification and optimization. Routinely, compounds are selected and progressed on the basis of their potency, a measure composed of both affinity and cooperativity. Affinity is generally a secondary measure, estimated from either inhibition of a radiolabelled allosteric modulator or from interactions with an orthosteric radioligand. For the vast majority of GPCRs, orthosteric and allosteric radioligands have yet to be developed, and an easily employed framework for quantification of allosteric behaviors is necessary to estimate allosteric modulator affinity and cooperativity from functional assays. Herein, we have validated the use of the operational model of allosterism (Leach et al., 2007) to derive estimates of allosteric modulator affinity and cooperativity for a representative class C GPCR, $mGlu_5$. Eleven chemical scaffolds were assessed for their interactions with glutamate, included compounds spanning from low to high affinity, varied in their degrees of positive and negative cooperativity, and also included allosteric agonists. The utility of the model for quantification of the impact of single amino acid substitutions on modulator cooperativity and affinity was exemplified. Moreover, we present a strategy to determine affinity from modulator concentration-response curves by incorporating the fold-shift at a set concentration as an estimate of cooperativity.

Allosteric modulators of $mGlu_5$ primarily influenced receptor function through modulation of efficacy (β). Specifically, there was no change in the affinity of representative PAMs or NAMs when assessing inhibition of [^{3}H]methoxyPEPy binding in the presence of 1 mM glutamate. Furthermore, we observed that PAM cooperativity

Molecular Pharmacology Fast Forward. Published on August 3, 2012 as DOI: 10.1124/mol.112.080531
This article has not been copyedited and formatted. The final version may differ from this version.

estimates were unaffected when making the assumption that $\alpha = 1$. Conceptually, efficacy modulation may arise from an increased affinity of intracellular signaling partners (G proteins, arrestins, etc.) for the conformations engendered by the ternary receptor-agonist-PAM complex compared to the binary receptor-agonist complex. Alternatively, the presence of PAMs may prevent receptor desensitization or other negative signaling outcomes, thereby resulting in enhancement of an agonist response. The lack of affinity modulation contrasts to what was observed by Bradley and colleagues (2011), where 30 μM quisqualate increased apparent PAM affinity when assessed in inhibition of [^{3}H]MPEP binding to cortical astrocytes and rat cortex preparations. Both 30 μM quisqualate and 1 mM glutamate would be expected to maximally occupy the available binding sites (~1000xK_A). The absence of affinity modulation observed with glutamate may be due to the probe-dependent nature of allosteric interactions or reflect context-dependent pharmacology between native tissue and HEK293 cells.

Strong correlation was observed between functional allosteric modulator affinity estimates and those from inhibition of [^{3}H]methoxyPEPy binding. Furthermore, functional affinity estimates also showed good correlation, indicative that affinity was independent of receptor expression level or the measure of receptor activation. Phenotypic differences in allosteric modulator pharmacology were observed. Agonism by PAMs and percent inhibition of the glutamate maximal response by certain NAMs differed depending upon receptor expression level and the assay of receptor function. Interestingly, glutamate showed lower efficacy in the high-expressing cell line for Ca^{2+} mobilization and for pERK1/2. Conversely, agonist PAMs, VU29 and CDPPB, showed the opposite profile, indicative of biased agonism. Increased receptor expression would

Molecular Pharmacology Fast Forward. Published on August 3, 2012 as DOI: 10.1124/mol.112.080531
This article has not been copyedited and formatted. The final version may differ from this version.

ordinarily be expected to increase agonist efficacy and/or potency (as observed for agonist PAMs). Clearly this is not the case for glutamate acting at $mGlu_5$ to mobilize intracellular Ca^{2+}. To interpret this disconnect for glutamate it is important to consider the overall potential impact of receptor overexpression on cellular responses beyond the established impact of increasing receptor reserve on potency of full agonists for GPCRs. Interestingly, the frequency of Ca^{2+} oscillations arising from $mGlu_5$ activation has been demonstrated to be receptor density dependent, resulting from a "dynamic uncoupling" mechanism whereby $mGlu_5$ undergoes cycles of rapid phosphorylation and dephosphorylation (Kawabata et al., 1996; Nash et al., 2002). It is conceivable that high $mGlu_5$ expression in HEK cells results in changes that ultimately negatively regulate Ca^{2+} mobilization, such as saturation of rate-limiting signaling partners, coupling to alternative pathways, altered phosphorylation, dimerization or other protein-protein interactions, desensitization or an increased number of uncoupled receptors at the cell surface. While multiple mechanisms are possible, further studies would be needed to evaluate this phenomenon and determine whether this is likely to be physiologically relevant under normal physiological or pathological conditions.

Notably, while affinities tended to be 3 fold higher, for all PAMs cooperativity (log β) was lower for pERK1/2 compared to Ca^{2+} mobilization. Furthermore, there was a lack of consensus between logβ values for positive allosteric modulation of Ca^{2+} mobilization in the low versus high-expressing cell lines. Interestingly, some PAMs showed greater agonist efficacy than glutamate in inducing pERK1/2 phosphorylation, suggesting that glutamate behaves as a partial agonist in stimulating this response. This suggests that the active receptor conformations, and therefore downstream signaling

Molecular Pharmacology Fast Forward. Published on August 3, 2012 as DOI: 10.1124/mol.112.080531
This article has not been copyedited and formatted. The final version may differ from this version.

events, engendered by PAMs are different than those induced by glutamate alone. Thus, the presence of $mGlu_5$ PAMs may bias $mGlu_5$ signaling towards increased ERK1/2 phosphorylation relative to calcium mobilization. While the detailed mechanisms underlying this are not fully understood, the possibility that $mGlu_5$ PAMs can induce changes in $mGlu_5$ signaling that differ from those observed with maximal glutamate is also consistent with the recent report that $mGlu_5$ PAMs promote increases in the frequency of Ca^{2+} oscillations to a greater extent than glutamate alone (Bradley et al., 2009). Mechanistically, $mGlu_5$-mediated Ca^{2+} mobilization and pERK1/2 can arise from independent signaling cascades in both neurons and recombinant cell lines (Thandi et al., 2002; Yang et al., 2006). Stimulus bias engendered by allosteric and orthosteric ligands of other family C GPCR family members, has recently been reported (Davey et al., 2011; Emery et al., 2012). If activation or inhibition of one pathway over another can be attributed to a specific disease state or therapeutic outcome, compound development could eventually be optimized for biased modulation (Kenakin & Miller 2010).

Traditionally, affinity determinations and confirmation of an allosteric mechanism of action has employed radioligand binding techniques, such as incomplete displacement and changes in the dissociation kinetics of an orthosteric radioligand (Ehlert, 1988). However, if an allosteric interaction is driven exclusively by efficacy modulation, as found here, these techniques cannot be used for detection. Quantification of affinity and cooperativity, without the need for a radioligand binding assay, presents a number of advantages. For GPCRs and binding sites for which radioligands are unavailable, including the majority of the mGlu family, the framework of the operational model of allosterism allows for optimization of affinity. Increasingly, drug discovery programs are

Molecular Pharmacology Fast Forward. Published on August 3, 2012 as DOI: 10.1124/mol.112.080531
This article has not been copyedited and formatted. The final version may differ from this version.

incorporating a need for verification of target engagement, largely through utilization of positron emission tomography (PET) to assess receptor occupancy of novel compounds at the desired site of action. We also described an approach to analyze PAM potency data, in combination with a maximal fold-shift experiment, to estimate modulator affinity. Since optimal radioligands and PET tracers show high affinity and specificity, such a method could easily be incorporated into established screening paradigms to inform chemistry efforts with respect to modulator affinity, allowing parallel identification of a lead compound and the needed tools to establish target engagement. Furthermore, affinity estimation would allow for correlation of *in vivo* parameters, such as minimal effective dose and unbound brain concentrations, with receptor occupancy and cooperativity.

In addition to informing SAR and lead optimization efforts, the ability to estimate affinity from functional assays enables delineation of effects on affinity and cooperativity within structure-function studies. Four previously identified point mutations were exemplified here for quantification of their impact on allosteric modulator interactions with $mGlu_5$. Val substitution of A809 and Y658 were previously reported to result in a loss of appreciable [^{3}H]MPEP binding and decreased MPEP potency (Pagano et al., 2000; Malherbe et al., 2003, 2006; Muhlemann et al., 2006), an effect attributed to a 100 fold reduction in MPEP affinity for the mutant receptors. L743V, reported to cause a 3 fold reduction in [^{3}H]MPEP affinity, was also assessed (Malherbe et al., 2003). As confirmation of the utility of the model for detecting mutational effects on affinity, L743V was found to decrease the MPEP functional affinity estimate by 3 fold. A809V and F585I also result in a loss of potentiation by PAMs, VU29 and CPPHA, respectively

Molecular Pharmacology Fast Forward. Published on August 3, 2012 as DOI: 10.1124/mol.112.080531
This article has not been copyedited and formatted. The final version may differ from this version.

(Chen et al., 2008), which could be due to decreased affinity and/or cooperativity. VU29 affinity was reduced 30 fold at A809V and CPPHA affinity was reduced 3 fold at F585I; neither mutation affected cooperativity of PAMs with glutamate. Interestingly, L743V enhanced VU29 cooperativity, while having no effect on affinity. Differential interactions with amino acids within a common binding site are likely to underscore potentiation versus inhibition, as well as contribute to pharmacological mode switches within distinct allosteric modulator scaffold. Further studies are ongoing to probe the molecular determinants of allosteric interactions at $mGlu_5$ and the interactions that govern affinity and cooperativity.

In validating the operational model of allosterism to quantify allosteric interactions at $mGlu_5$, we discovered evidence for signal bias by both "pure" and agonist PAMs of $mGlu_5$ when compared to glutamate. Furthermore, we describe a strategy to estimate affinity from PAM potency curves. Quantification of allosteric interactions provides the means to better interpret SAR, structure-function experiments and identify signal bias.

Molecular Pharmacology Fast Forward. Published on August 3, 2012 as DOI: 10.1124/mol.112.080531
This article has not been copyedited and formatted. The final version may differ from this version.

Acknowledgements

The authors wish to thank Julie R. Field for fruitful discussions and acknowledge the invaluable technical assistance of Kiran Gogi and Daryl Venable.

Molecular Pharmacology Fast Forward. Published on August 3, 2012 as DOI: 10.1124/mol.112.080531
This article has not been copyedited and formatted. The final version may differ from this version.

Authorship Contributions

Participated in research design: Conn, Gregory, Niswender, Noetzel, Rodriguez, Rook, Vinson

Conducted experiments: Gregory, Noetzel, Rook, Vinson

Contributed new reagents: Chauder, Chun, Emmitte, Felts, Lindsley, Stauffer, Zhou

Performed data analysis: Gregory, Noetzel, Rook, Vinson

Wrote or contributed to writing of manuscript: Conn, Gregory, Niswender

Molecular Pharmacology Fast Forward. Published on August 3, 2012 as DOI: 10.1124/mol.112.080531
This article has not been copyedited and formatted. The final version may differ from this version.

References

Alagille D, DaCosta H, Chen Y, Hemstapat K, Rodriguez A, Baldwin RM, Conn PJ and Tamagnan GD (2011) Potent mGluR5 antagonists: pyridyl and thiazolyl-ethynyl-3,5-disubstituted-phenyl series. *Bioorg Med Chem Lett* **21**(11): 3243-3247.

Bradley SJ, Watson JM and Challiss RA (2009) Effects of positive allosteric modulators on single-cell oscillatory Ca2+ signaling initiated by the type 5 metabotropic glutamate receptor. *Mol Pharmacol* **76**(6): 1302-1313.

Bradley SJ, Langmead CJ, Watson JM and Challiss RA (2011) Quantitative analysis reveals multiple mechanisms of allosteric modulation of the mGlu5 receptor in rat astroglia. *Mol Pharmacol* **79**(5): 874-885.

Chen Y, Goudet C, Pin JP and Conn PJ (2008) N-{4-Chloro-2-[(1,3-dioxo-1,3-dihydro-2H-isoindol-2-yl)methyl]phenyl}-2-hy droxybenzamide (CPPHA) acts through a novel site as a positive allosteric modulator of group 1 metabotropic glutamate receptors. *Mol Pharmacol* **73**(3): 909-918.

Chen Y, Nong Y, Goudet C, Hemstapat K, de Paulis T, Pin JP and Conn PJ (2007) Interaction of novel positive allosteric modulators of metabotropic glutamate receptor 5 with the negative allosteric antagonist site is required for potentiation of receptor responses. *Mol Pharmacol* **71**(5): 1389-1398.

Cheng Y and Prusoff WH (1973) Relationship between the inhibition constant (K1) and the concentration of inhibitor which causes 50 per cent inhibition (I50) of an enzymatic reaction. *Biochemical pharmacology* **22**(23): 3099-3108.

Chua PC, Nagasawa JY, Bleicher LS, Munoz B, Schweiger EJ, Tehrani L, Anderson JJ, Cramer M, Chung J, Green MD, King CD, Reyes-Manalo G and Cosford ND (2005)

Cyclohexenyl- and dehydropiperidinyl-alkynyl pyridines as potent metabotropic glutamate subtype 5 (mGlu5) receptor antagonists. *Bioorg Med Chem Lett* **15**(20): 4589-4593.

Cosford ND, Tehrani L, Roppe J, Schweiger E, Smith ND, Anderson J, Bristow L, Brodkin J, Jiang X, McDonald I, Rao S, Washburn M and Varney MA (2003a) 3-[(2-Methyl-1,3-thiazol-4-yl)ethynyl]-pyridine: a potent and highly selective metabotropic glutamate subtype 5 receptor antagonist with anxiolytic activity. *J Med Chem* **46**(2): 204-206.

Cosford ND, Roppe J, Tehrani L, Schweiger EJ, Seiders TJ, Chaudary A, Rao S and Varney MA (2003b) [3H]-methoxymethyl-MTEP and [3H]-methoxy-PEPy: potent and selective radioligands for the metabotropic glutamate subtype 5 (mGlu5) receptor. *Bioorg Med Chem Lett* **13**(3): 351-354.

Davey AE, Leach K, Valant C, Conigrave AD, Sexton PM and Christopoulos A (2012) Positive and negative allosteric modulators promote biased signaling at the calcium-sensing receptor. *Endocrinology* **153**(3): 1232-1241.

de Paulis T, Hemstapat K, Chen Y, Zhang Y, Saleh S, Alagille D, Baldwin RM, Tamagnan GD and Conn PJ (2006) Substituent effects of N-(1,3-diphenyl-1H-pyrazol-5-yl)benzamides on positive allosteric modulation of the metabotropic glutamate-5 receptor in rat cortical astrocytes. *J Med Chem* **49**(11): 3332-3344.

Ehlert FJ (1988) Estimation of the affinities of allosteric ligands using radioligand binding and pharmacological null methods. *Mol Pharmacol* **33**(2): 187-194.

Emery AC, Diraddo JO, Miller E, Hathaway HA, Pshenichkin S, Takoudjou GR, Grajkowska E, Yasuda RP, Wolfe BB and Wroblewski J (2012) Ligand Bias at Metabotropic Glutamate 1a Receptor: Molecular Determinants that Distinguish beta-arrestin from G Protein

Mediated Signaling. *Mol Pharmacol*.

Felts AS, Lindsley SR, Lamb JP, Rodriguez AL, Menon UN, Jadhav S, Jones CK, Conn PJ, Lindsley CW and Emmitte KA (2010) 3-Cyano-5-fluoro-N-arylbenzamides as negative allosteric modulators of mGlu(5): Identification of easily prepared tool compounds with CNS exposure in rats. *Bioorg Med Chem Lett* **20**(15): 4390-4394.

Felts AS, Saleh SA, Le U, Rodriguez AL, Weaver CD, Conn PJ, Lindsley CW and Emmitte KA (2009) Discovery and SAR of 6-substituted-4-anilinoquinazolines as non-competitive antagonists of mGlu5. *Bioorg Med Chem Lett* **19**(23): 6623-6626.

Galambos J, Wagner G, Nogradi K, Bielik A, Molnar L, Bobok A, Horvath A, Kiss B, Kolok S, Nagy J, Kurko D, Bakk ML, Vastag M, Saghy K, Gyertyan I, Gal K, Greiner I, Szombathelyi Z, Keseru GM and Domany G (2010) Carbamoyloximes as novel non-competitive mGlu5 receptor antagonists. *Bioorg Med Chem Lett* **20**(15): 4371-4375.

Gasparini F, Lingenhohl K, Stoehr N, Flor PJ, Heinrich M, Vranesic I, Biollaz M, Allgeier H, Heckendorn R, Urwyler S, Varney MA, Johnson EC, Hess SD, Rao SP, Sacaan AI, Santori EM, Velicelebi G and Kuhn R (1999) 2-Methyl-6-(phenylethynyl)-pyridine (MPEP), a potent, selective and systemically active mGlu5 receptor antagonist. *Neuropharmacology* **38**(10): 1493-1503.

Gilbert AM, Bursavich MG, Lombardi S, Adedoyin A, Dwyer JM, Hughes Z, Kern JC, Khawaja X, Rosenzweig-Lipson S, Moore WJ, Neal SJ, Olsen M, Rizzo SJ and Springer D (2011) 3-(Pyridin-2-yl-ethynyl)benzamide metabotropic glutamate receptor 5 negative allosteric modulators: hit to lead studies. *Bioorg Med Chem Lett* **21**(1): 195-199.

Gregory KJ, Sexton PM and Christopoulos A (2010) Overview of Receptor Allosterism, in *Current Protoc Pharmacol* Wiley Interscience Chapter 1:Unit 1.21.

Hammond AS, Rodriguez AL, Townsend SD, Niswender CM, Gregory KJ, Lindsley CW and Conn PJ (2010) Discovery of a Novel Chemical Class of mGlu(5) Allosteric Ligands with Distinct Modes of Pharmacology. *ACS Chem Neurosci* **1**(10): 702-716.

Huang D, Poon SF, Chapman DF, Chung J, Cramer M, Reger TS, Roppe JR, Tehrani L, Cosford ND and Smith ND (2004) 2-(2-[3-(pyridin-3-yloxy)phenyl]-2H-tetrazol-5-yl) pyridine: a highly potent, orally active, metabotropic glutamate subtype 5 (mGlu5) receptor antagonist. *Bioorg Med Chem Lett* **14**(22): 5473-5476.

Jaeschke G, Porter R, Buttelmann B, Ceccarelli SM, Guba W, Kuhn B, Kolczewski S, Huwyler J, Mutel V, Peters JU, Ballard T, Prinssen E, Vieira E, Wichmann J and Spooren W (2007) Synthesis and biological evaluation of fenobam analogs as mGlu5 receptor antagonists. *Bioorg Med Chem Lett* **17**(5): 1307-1311.

Kawabata S, Tsutsumi R, Kohara A, Yamaguchi T, Nakanishi S and Okada M (1996) Control of calcium oscillations by phosphorylation of metabotropic glutamate receptors. *Nature* **383**(6595): 89-92.

Kenakin T and Miller LJ (2010) Seven transmembrane receptors as shapeshifting proteins: the impact of allosteric modulation and functional selectivity on new drug discovery. *Pharmacol Rev* **62**(2): 265-304.

Kinney GG, O'Brien JA, Lemaire W, Burno M, Bickel DJ, Clements MK, Chen TB, Wisnoski DD, Lindsley CW, Tiller PR, Smith S, Jacobson MA, Sur C, Duggan ME, Pettibone DJ, Conn PJ and Williams DL, Jr. (2005) A novel selective positive allosteric modulator of metabotropic glutamate receptor subtype 5 has in vivo activity and antipsychotic-like effects in rat behavioral models. *J Pharmacol Exp Ther* **313**(1): 199-206.

Kulkarni SS, Nightingale B, Dersch CM, Rothman RB and Newman AH (2006) Design and

synthesis of noncompetitive metabotropic glutamate receptor subtype 5 antagonists. *Bioorg Med Chem Lett* **16**(13): 3371-3375.

Kulkarni SS, Zou MF, Cao J, Deschamps JR, Rodriguez AL, Conn PJ and Newman AH (2009) Structure-activity relationships comparing N-(6-methylpyridin-yl)-substituted aryl amides to 2-methyl-6-(substituted-arylethynyl)pyridines or 2-methyl-4-(substituted-arylethynyl)thiazoles as novel metabotropic glutamate receptor subtype 5 antagonists. *J Med Chem* **52**(11): 3563-3575.

Lazareno S and Birdsall N (1995) Detection, quantitation, and verification of allosteric interactions of agents with labeled and unlabeled ligands at G protein-coupled receptors: interactions of strychnine and acetylcholine at muscarinic receptors. *Mol Pharmacol* **48**(2): 362-378.

Leach K, Sexton PM and Christopoulos A (2007) Allosteric GPCR modulators: taking advantage of permissive receptor pharmacology. *Trends in Pharmacol Sci* **28**(8): 382-389.

Lindemann L, Jaeschke G, Michalon A, Vieira E, Honer M, Spooren W, Porter R, Hartung T, Kolczewski S, Buttelmann B, Flament C, Diener C, Fischer C, Gatti S, Prinssen EP, Parrott N, Hoffmann G and Wettstein JG (2011) CTEP: a novel, potent, long-acting, and orally bioavailable metabotropic glutamate receptor 5 inhibitor. *J Pharmacol Exp Ther* **339**(2): 474-486.

Liu F, Grauer S, Kelley C, Navarra R, Graf R, Zhang G, Atkinson PJ, Popiolek M, Wantuch C, Khawaja X, Smith D, Olsen M, Kouranova E, Lai M, Pruthi F, Pulicicchio C, Day M, Gilbert A, Pausch MH, Brandon NJ, Beyer CE, Comery TA, Logue S, Rosenzweig-Lipson S and Marquis KL (2008) ADX47273 [S-(4-fluoro-phenyl)-{3-[3-(4-fluoro-phenyl)-[1,2,4]-oxadiazol-5-yl]-piperidin-1- yl}-methanone]: a novel metabotropic

glutamate receptor 5-selective positive allosteric modulator with preclinical antipsychotic-like and procognitive activities. *J Pharmacol Exp Ther* **327**(3): 827-839.

Malherbe P, Kratochwil N, Muhlemann A, Zenner M-T, Fischer C, Stahl M, Gerber PR, Jaeschke G and Porter RHP (2006) Comparison of the binding pockets of two chemically unrelated allosteric antagonists of the mGlu5 receptor and identification of crucial residues involved in the inverse agonism of MPEP. *J Neurochem* **98**(2): 601-615.

Malherbe P, Kratochwil N, Zenner MT, Piussi J, Diener C, Kratzeisen C, Fischer C and Porter RH (2003) Mutational analysis and molecular modeling of the binding pocket of the metabotropic glutamate 5 receptor negative modulator 2-methyl-6-(phenylethynyl)-pyridine. *Mol Pharmacol* **64**(4): 823-832.

Melancon BJ, Hopkins CR, Wood MR, Emmitte KA, Niswender CM, Christopoulos A, Conn PJ and Lindsley CW (2012) Allosteric modulation of seven transmembrane spanning receptors: theory, practice, and opportunities for central nervous system drug discovery. *J Med Chem* **55**(4): 1445-1464.

Milbank JB, Knauer CS, Augelli-Szafran CE, Sakkab-Tan AT, Lin KK, Yamagata K, Hoffman JK, Zhuang N, Thomas J, Galatsis P, Wendt JA, Mickelson JW, Schwarz RD, Kinsora JJ, Lotarski SM, Stakich K, Gillespie KK, Lam WW and Mutlib AE (2007) Rational design of 7-arylquinolines as non-competitive metabotropic glutamate receptor subtype 5 antagonists. *Bioorg Med Chem Lett* **17**(16): 4415-4418.

Mueller R, Dawson ES, Meiler J, Rodriguez AL, Chauder BA, Bates BS, Felts AS, Lamb JP, Menon UN, Jadhav SB, Kane AS, Jones CK, Gregory KJ, Niswender CM, Conn PJ, Olsen CM, Winder DG, Emmitte KA and Lindsley CW (2012) Discovery of 2-(2-benzoxazoyl amino)-4-aryl-5-cyanopyrimidine as negative allosteric modulators (NAMs)

of metabotropic glutamate receptor 5 (mGlu(5)): from an artificial neural network virtual screen to an in vivo tool compound. *ChemMedChem* **7**(3): 406-414.

Muhlemann A, Ward NA, Kratochwil N, Diener C, Fischer C, Stucki A, Jaeschke G, Malherbe P and Porter RH (2006) Determination of key amino acids implicated in the actions of allosteric modulation by 3,3'-difluorobenzaldazine on rat mGlu5 receptors. *Eur J Pharmacol* **529**(1-3): 95-104.

Mutel V, Ellis GJ, Adam G, Chaboz S, Nilly A, Messer J, Bleuel Z, Metzler V, Malherbe P, Schlaeger EJ, Roughley BS, Faull RL and Richards JG (2000) Characterization of [(3)H]Quisqualate binding to recombinant rat metabotropic glutamate 1a and 5a receptors and to rat and human brain sections. *J Neurochem* **75**(6): 2590-2601.

Nash MS, Schell MJ, Atkinson PJ, Johnston NR, Nahorski SR and Challiss RA (2002) Determinants of metabotropic glutamate receptor-5-mediated Ca2+ and inositol 1,4,5-trisphosphate oscillation frequency. Receptor density versus agonist concentration. *The Journal of biological chemistry* **277**(39): 35947-35960.

Niswender CM and Conn PJ (2010) Metabotropic glutamate receptors: physiology, pharmacology, and disease. *Annu Rev Pharmacol Toxicol* **50**: 295-322.

Noetzel MJ, Rook JM, Vinson PN, Cho HP, Days E, Zhou Y, Rodriguez AL, Lavreysen H, Stauffer SR, Niswender CM, Xiang Z, Daniels JS, Jones CK, Lindsley CW, Weaver CD and Conn PJ (2012) Functional impact of allosteric agonist activity of selective positive allosteric modulators of metabotropic glutamate receptor subtype 5 in regulating central nervous system function. *Mol Pharmacol* **81**(2): 120-133.

O'Brien JA, Lemaire W, Wittmann M, Jacobson MA, Ha SN, Wisnoski DD, Lindsley CW, Schaffhauser HJ, Rowe B, Sur C, Duggan ME, Pettibone DJ, Conn PJ and Williams DL,

Jr. (2004) A novel selective allosteric modulator potentiates the activity of native metabotropic glutamate receptor subtype 5 in rat forebrain. *J Pharmacol Exp Ther* **309**(2): 568-577.

Pagano A, Ruegg D, Litschig S, Stoehr N, Stierlin C, Heinrich M, Floersheim P, Prezeau L, Carroll F, Pin JP, Cambria A, Vranesic I, Flor PJ, Gasparini F and Kuhn R (2000) The non-competitive antagonists 2-methyl-6-(phenylethynyl)pyridine and 7-hydroxyiminocyclopropan[b]chromen-1a-carboxylic acid ethyl ester interact with overlapping binding pockets in the transmembrane region of group I metabotropic glutamate receptors. *J Biol Chem* **275**(43): 33750-33758.

Poon SF, Eastman BW, Chapman DF, Chung J, Cramer M, Holtz G, Cosford ND and Smith ND (2004) 3-[3-Fluoro-5-(5-pyridin-2-yl-2H-tetrazol-2-yl)phenyl]-4-methylpyridine: a highly potent and orally bioavailable metabotropic glutamate subtype 5 (mGlu5) receptor antagonist. *Bioorg Med Chem Lett* **14**(22): 5477-5480.

Rodriguez AL, Grier MD, Jones CK, Herman EJ, Kane AS, Smith RL, Williams R, Zhou Y, Marlo JE, Days EL, Blatt TN, Jadhav S, Menon UN, Vinson PN, Rook JM, Stauffer SR, Niswender CM, Lindsley CW, Weaver CD and Conn PJ (2010) Discovery of novel allosteric modulators of metabotropic glutamate receptor subtype 5 reveals chemical and functional diversity and in vivo activity in rat behavioral models of anxiolytic and antipsychotic activity. *Mol Pharmacol* **78**(6): 1105-1123.

Rodriguez AL, Nong Y, Sekaran NK, Alagille D, Tamagnan GD and Conn PJ (2005) A close structural analog of 2-methyl-6-(phenylethynyl)-pyridine acts as a neutral allosteric site ligand on metabotropic glutamate receptor subtype 5 and blocks the effects of multiple allosteric modulators. *Mol Pharmacol* **68**(6): 1793-1802.

Rodriguez AL, Williams R, Zhou Y, Lindsley SR, Le U, Grier MD, Weaver CD, Conn PJ and Lindsley CW (2009) Discovery and SAR of novel mGluR5 non-competitive antagonists not based on an MPEP chemotype. *Bioorg Med Chem Lett* **19**(12): 3209-3213.

Roppe J, Smith ND, Huang D, Tehrani L, Wang B, Anderson J, Brodkin J, Chung J, Jiang X, King C, Munoz B, Varney MA, Prasit P and Cosford ND (2004) Discovery of novel heteroarylazoles that are metabotropic glutamate subtype 5 receptor antagonists with anxiolytic activity. *J Med Chem* **47**(19): 4645-4648.

Sams AG, Mikkelsen GK, Brodbeck RM, Pu X and Ritzen A (2011) Efficacy switching SAR of mGluR5 allosteric modulators: highly potent positive and negative modulators from one chemotype. *Bioorg Med Chem Lett* **21**(11): 3407-3410.

Tehrani LR, Smith ND, Huang D, Poon SF, Roppe JR, Seiders TJ, Chapman DF, Chung J, Cramer M and Cosford ND (2005) 3-[Substituted]-5-(5-pyridin-2-yl-2H-tetrazol-2-yl)benzonitriles: identification of highly potent and selective metabotropic glutamate subtype 5 receptor antagonists. *Bioorg Med Chem Lett* **15**(22): 5061-5064.

Thandi S, Blank JL and Challiss RA (2002) Group-I metabotropic glutamate receptors, mGlu1a and mGlu5a, couple to extracellular signal-regulated kinase (ERK) activation via distinct, but overlapping, signalling pathways. *J Neurochem* **83**(5): 1139-1153.

Vanejevs M, Jatzke C, Renner S, Muller S, Hechenberger M, Bauer T, Klochkova A, Pyatkin I, Kazyulkin D, Aksenova E, Shulepin S, Timonina O, Haasis A, Gutcaits A, Parsons CG, Kauss V and Weil T (2008) Positive and negative modulation of group I metabotropic glutamate receptors. *J Med Chem* **51**(3): 634-647.

Varney MA, Cosford ND, Jachec C, Rao SP, Sacaan A, Lin FF, Bleicher L, Santori EM, Flor PJ, Allgeier H, Gasparini F, Kuhn R, Hess SD, Velicelebi G and Johnson EC (1999) SIB-

1757 and SIB-1893: selective, noncompetitive antagonists of metabotropic glutamate receptor type 5. *J Pharmacol Exp Ther* **290**(1): 170-181.

Wagner G, Weber C, Nyeki O, Nogradi K, Bielik A, Molnar L, Bobok A, Horvath A, Kiss B, Kolok S, Nagy J, Kurko D, Gal K, Greiner I, Szombathelyi Z, Keseru GM and Domany G (2010) Hit-to-lead optimization of disubstituted oxadiazoles and tetrazoles as mGluR5 NAMs. *Bioorg Med Chem Lett* **20**(12): 3737-3741.

Weiss JM, Jimenez HN, Li G, April M, Uberti MA, Bacolod MD, Brodbeck RM and Doller D (2011) 6-Aryl-3-pyrrolidinylpyridines as mGlu5 receptor negative allosteric modulators. *Bioorg Med Chem Lett* **21**(16): 4891-4899.

Wood MR, Hopkins CR, Brogan JT, Conn PJ and Lindsley CW (2011) "Molecular switches" on mGluR allosteric ligands that modulate modes of pharmacology. *Biochemistry* **50**(13): 2403-2410.

Yang L, Mao L, Chen H, Catavsan M, Kozinn J, Arora A, Liu X and Wang JQ (2006) A signaling mechanism from G alpha q-protein-coupled metabotropic glutamate receptors to gene expression: role of the c-Jun N-terminal kinase pathway. *J Neurosci* **26**(3): 971-980.

Zhang P, Zou MF, Rodriguez AL, Conn PJ and Newman AH (2010) Structure-activity relationships in a novel series of 7-substituted-aryl quinolines and 5-substituted-aryl benzothiazoles at the metabotropic glutamate receptor subtype 5. *Bioorg Med Chem* **18**(9): 3026-3035.

Zhou Y, Manka JT, Rodriguez AL, Weaver CD, Days EL, Vinson PN, Jadhav S, Hermann EJ, Jones CK, Conn PJ, Lindsley CW and Stauffer SR (2010) Discovery of N-Aryl Piperazines as Selective mGluR5 Potentiators with Improved In Vivo Utility. *ACS*

Medicinal Chemistry Letters **1**(8): 433-438.

Zou MF, Cao J, Rodriguez AL, Conn PJ and Newman AH (2011) Design and synthesis of substituted N-(1,3-diphenyl-1H-pyrazol-5-yl)benzamides as positive allosteric modulators of the metabotropic glutamate receptor subtype 5. *Bioorg Med Chem Lett* **21**(9): 2650-2654.

Footnotes

a) This work is supported by the National Institute of Mental Health [Grant 2R01 MH062646-13]; National Institute of Neurological Disorders and Stroke [Grant 2R01NS031373-16A2]; National Institute of Drug Abuse [Grant 1R01DA023947]; Molecular Libraries Probe Production Centers Network [Grant 5 u54 MH84659-03, 5 u54 MH84659-03S1]; National Research Service Awards from National Institute of Neurological Disorders and Stroke [MJN: F32 NS071746] and National Institute of Mental Health [JMR: F32 MH088234-02]; NARSAD Maltz Investigator Award 2010 (KJG); American Australian Association Merck Foundation Fellowship 2010 (KJG); National Health and Medical Research Council (Australia) Overseas Biomedical Postdoctoral Training Fellowship (KJG). The content is solely the responsibility of the authors and does not necessarily represent the official view of the organizations listed above.

b) This work was presented in abstract form:

Karen J. Gregory, E.N. Dong, S.D. Reiff, J.M. Rook, M.J. Noetzel, H.C. Plumley, K.W. Kaufmann, J.T. Manka, Y.S. Zhou, P.N. Vinson, S.R. Stauffer, C.M. Niswender, C.W. Lindsley, J. Meiler and P.J. Conn "Application of an operational model of allosterism to investigate the structural determinants of metabotropic glutamate receptor 5 allosteric modulation" 7th International Meeting on Metabotropic Glutamate Receptors, Taormina, Italy (October 2011).

c) PJC is a consultant for Seaside Therapeutic and receives research support from Seaside Therapeutics and Johnson and Johnson/Janssen Pharmaceutica.

d) Reprint Requests should be addressed to P. Jeffrey Conn, Department of Pharmacology & Vanderbilt Center for Neuroscience Drug Discovery, Vanderbilt University Medical Center, 1215 Light Hall, 2215-B Garland Ave, Nashville, TN, USA, 37232-0697; jeff.conn@vanderbilt.edu

Molecular Pharmacology Fast Forward. Published on August 3, 2012 as DOI: 10.1124/mol.112.080531
This article has not been copyedited and formatted. The final version may differ from this version.

Figure Legends

Figure 1 Allosteric modulator potency is influenced by agonist concentration, modulator affinity and cooperativity

A) Simulation of the effect of different agonist concentrations on the potency of a negative allosteric modulator, where EC100** indicates an agonist concentration 30X in excess of that required to elicit a maximal response. **B**) Simulation of the effect of different agonist concentrations on the potency of a positive allosteric modulator. **C**) Literature survey of $mGlu_5$ NAM potency and affinity estimates, the dashed line represents unity, the dotted line indicates modulators whose potency and affinity lie within 3-fold of each other, the solid line indicates a 10-fold deviation. **D**) Literature survey of $mGlu_5$ PAM potency and affinity estimates. (Data shown in **C** and **D** taken from: Huang et al., 2004; Poon et al., 2004; Roppe et al., 2004; Chua et al., 2005; Tehrani et al., 2005; dePaulis et al., 2006; Kulkarni et al., 2006 & 2009; Jaeschke et al., 2007; Milbank et al., 2007; Liu et al., 2008; Vanejevs et al., 2008; Felts et al., 2009 & 2010; Galambos et al., 2010; Rodriguez et al., 2010; Wagner et al., 2010; Zhang et al., 2010; Alagille et al., 2011; Gilbert et al., 2011; Lindemann et al., 2011; Sams et al., 2011; Weiss et al., 2011; Zou et al., 2011; Mueller et al., 2012)

Figure 2 Structures of $mGlu_5$ allosteric modulators included in this study

VU0366248 and VU0366249 were originally reported as compound 41 and 42, respectively in Felts et al., 2010.

Figure 3 Inhibition of [^{3}H]methoxyPEPy binding to HEK293A-$mGlu_5$-wt cell membranes

Data represent the mean ± s.e.m. from a minimum of three independent determinations.

Molecular Pharmacology Fast Forward. Published on August 3, 2012 as DOI: 10.1124/mol.112.080531
This article has not been copyedited and formatted. The final version may differ from this version.

Figure 4 Allosteric modulation of glutamate concentration-response curves for Ca^{++} mobilization in the low-expressing HEK293A-$mGlu_5$ cell line.

In the low-expressing HEK293A-$mGlu_5$-wt cell line, CPPHA (**A**) and CDPPB (**B**) induce a leftward shift in the glutamate concentration-response curve (crc) for intracellular Ca^{2+} mobilization with no change in the maximal response. MPEP (**C**) VU0366249 (**D**) and M-5MPEP (**E**) inhibit glutamate-stimulated intracellular Ca^{2+} mobilization. **F**) Comparison of modulator affinity estimates when determining either the composite cooperativity parameter αβ for PAMs (closed circles) and allowing α to float for NAMs (open circles) (x-axis) or assuming α=1 and calculating logβ (y-axis). **G**) Calculated cooperativity estimates, the assumption that α=1, has no effect on the apparent cooperativity between glutamate and PAMs (closed circles) and weak NAMs (open circles). **H**) Comparison of affinity estimates for PAMs (closed circles) and NAMs (open circles) from radioligand binding (x-axis) and Ca^{2+} mobilization assay (y-axis) in the low-expressing HEK293A-$mGlu_5$ cells. In panels **F-H**, the dashed line represents unity. Data represent the mean ± s.e.m. from a minimum of three independent determinations. Error bars not shown lie within the dimensions of the symbol.

Figure 5 Allosteric modulation of glutamate concentration-response curves for Ca^{++} mobilization in the high-expressing HEK293-$mGlu_5$ cell line.

In the high-expressing $mGlu_5$ HEK293 cell line, increased agonist activity is seen for CPPHA (**A**) and CDPPB (**B**) as well as induction of a leftward shift in the glutamate crc for Ca^{2+} mobilization. MPEP (**C**), VU0366249 (**D**) and M-5MPEP (**E**) inhibit glutamate stimulation of Ca^{2+} mobilization. **F**) Comparison of affinity estimates for NAMs (open circles) and PAMs (closed circles) from the Ca^{2+} mobilization assay in low (x-axis)

Molecular Pharmacology Fast Forward. Published on August 3, 2012 as DOI: 10.1124/mol.112.080531
This article has not been copyedited and formatted. The final version may differ from this version.

versus high (y-axis) expressing $mGlu_5$ cell lines, where the dashed line represents unity. Data represent the mean ± s.e.m. from a minimum of three independent determinations. Error bars not shown lie within the dimensions of the symbol.

Figure 6 Allosteric modulation of glutamate concentration-response curves for ERK1/2 phosphorylation in the low-expressing HEK293A-$mGlu_5$ cell line.

In the low-expressing cell line, CPPHA (**A**) and CDPPB (**B**) display agonist activity and potentiate the glutamate crc for phosphorylation of ERK1/2. MPEP (**C**), VU0366249 (**D**) and M-5MPEP (**E**) inhibit the glutamate stimulated phosphorylation of ERK1/2. **F**) Comparison of affinity estimates for PAMs (closed circles) and NAMs (open circles) in the low-expressing cell line determined from pERK1/2 (y-axis) and Ca^{2+} mobilization assays (x-axis), where the dashed line represents unity. Data represent the mean ± s.e.m. from a minimum of three independent determinations. Error bars not shown lie within the dimensions of the symbol.

Figure 7 Effect of single point mutations on MPEP inhibition of $mGlu_5$-mediated Ca^{2+} mobilization in response to glutamate

Translocation of glutamate crc in the presence of indicated concentrations of MPEP at polyclonal HEK293A-$mGlu_5$ cells expressing wild type (**A**), Y658V (**B**), L743V (**C**) and A809V (**D**). Data represent the mean ±s.e.m. from a minimum of three independent determinations. Error bars not shown lie within the dimensions of the symbol.

Figure 8 Effect of single point mutations of potentiation of $mGlu_5$-mediated Ca^{2+} mobilization in response to glutamate by VU29 and CPPHA

Translocation of glutamate crc in the presence of indicated concentrations of VU29 at the polyclonal HEK293A-$mGlu_5$ cells expressing wild type (**A**) and A809V (**B**). Potentiation

Molecular Pharmacology Fast Forward. Published on August 3, 2012 as DOI: 10.1124/mol.112.080531
This article has not been copyedited and formatted. The final version may differ from this version.

of the glutamate crc for Ca^{2+} mobilization by indicated concentrations of CPPHA in polyclonal HEK293A-$mGlu_5$ cells expressing wild type (**C**) and F585I (**D**). Data represent the mean ±s.e.m. from a minimum of three independent determinations. Error bars not shown lie within the dimensions of the symbol.

Figure 9 Estimation of allosteric modulator cooperativity and affinity from potency curves

Allosteric modulator potency curves for indicated positive allosteric modulators (**A** & **B**) in the presence of EC_{20} glutamate. CPPHA and VU0364289 both achieved the maximal response to glutamate and thus logβ values were constrained to equal the average maximal leftward shift caused in the glutamate crc (Table 6) to estimate pK_B. For all other PAMs, both logβ and pK_B values were determined by non-linear regression. Negative allosteric modulators were assessed for their ability to inhibit a sub maximal glutamate response (**C**). Affinity estimates from potency curves (y-axis) and from progressive fold-shift analysis (x-axis) for PAMs (closed circles) and NAM (open circles) show strong correlation (**D**). Similarly, strong correlation was observed between logβ values (**E**) estimated by non-linear regression from modulator potency curves (y-axis) and from progressive fold-shift analysis (x-axis). Data represent the mean ±s.e.m. from a minimum of three independent determinations. Error bars not shown lie within the dimensions of the symbol. Dashed line corresponds to unity.

Molecular Pharmacology Fast Forward. Published on August 3, 2012 as DOI: 10.1124/mol.112.080531
This article has not been copyedited and formatted. The final version may differ from this version.

Table 1: Summary of affinity (K_I) and cooperativity (α) estimates for $mGlu_5$ allosteric modulators determined from [^{3}H]methoxyPEPy inhibition binding assays. Data represent the mean and s.e.m from a minimum of three independent determinations.

	pK_I[a] (log α)[b]	pK_I (log α) + 1mM glutamate[c]
CDPPB	6.65 ±0.11	n.d.
VU29	6.69 ±0.10 (-0.95 ±0.01)	7.20 ±0.21 (-0.96 ±0.05)
CPPHA	5.52 ±0.06 (-0.64 ±0.02)	5.92 ±0.21 (-0.62 ±0.01)
VU0357121	5.65 ±0.19 (-0.24 ±0.01)	5.78 ±0.20 (-0.35 ±0.04)
VU0364289	4.82 ±0.15	5.26 ±0.21
VU0092273	5.97 ±0.09	n.d.
VU0360172	6.55 ±0.03 (-1.21 ±0.17)	6.75 ±0.07 (-1.39 ±0.09)
VU0405398	6.60 ±0.14	n.d.
VU0415051	6.88 ±0.04	n.d.
VU0405386	7.98 ±0.05	8.31 ±0.14
MPEP	8.00 ±0.04	8.26 ±0.10
M-5MPEP	6.89 ±0.16	n.d.
VU0285683	7.68 ±0.04	7.60 ±0.07
VU0366248	6.18 ±0.06	6.39 ±0.10
VU0366249	5.55 ±0.08	n.d.
VU0366058	6.92 ±0.06	6.83 ±0.13

[#] modulators that did not fully displace [^{3}H]methoxyPEPy were fitted with an allosteric model to derive affinity and cooperativity estimates (equation 1).
[a] negative logarithm of the equilibrium dissociation constant determined by nonlinear regression of [^{3}H]methoxyPEPy binding.
[b] logarithm of the cooperativity factor for the interaction between the indicated allosteric modulator and [^{3}H]methoxyPEPy.
[c] allosteric modulator affinity estimates were not significantly different ($p<0.05$) in the presence of 1mM glutamate using one-way ANOVA with Tukey's post-test.
n.d. denotes not determined.

Table 2: Summary of operational model parameters for positive allosteric modulation of glu-mediated intracellular Ca^{2+} mobilization using HEK cells expressing either low or high levels of $mGlu_5$. Data represent the mean and s.e.m from a minimum of three independent determinations.

	HEK293A-$mGlu_5$ (low): determining composite cooperativity ($\alpha\beta$)									
	CDPPB	VU29	CPPHA	VU0357121	VU0364289	VU0092273	VU0360172	VU0405398	VU0415051	VU0405386
pK_B[a]	6.31 ±0.10	6.20 ±0.09	6.03 ±0.10	6.46 ±0.09	5.18 ±0.13	6.45 ±0.11	6.98 ±0.05	7.30 ±0.24	7.45 ±0.24	8.17 ±0.24
$log\alpha\beta$[b]	0.78 ±0.16	0.81 ±0.08	0.65 ±0.09	0.42 ±0.05	0.97 ±0.08	0.49 ±0.04	0.51 ±0.02	0.33 ±0.04	0.36 ±0.06	0.60 ±0.11
$log\tau_B$[c]	-0.42 ±0.23	-0.67 ±0.06	n.a.	n.a.	n.a.	n.a.	n.a.	n.a.	n.a.	n.a.
	HEK293A-$mGlu_5$ (low): assuming neutral affinity cooperativity (α=1)									
	CDPPB	VU29	CPPHA	VU0357121	VU0364289	VU0092273	VU0360172	VU0405398	VU0415051	VU0405386
pK_B	6.38 ±0.10	6.23 ±0.09	6.06 ±0.10	6.48 ±0.17	5.22 ±0.16	6.46 ±0.12	7.00 ±0.05	7.29 ±0.26	7.46 ±0.20	8.18 ±0.28
$log\beta$[d]	0.66 ±0.15	0.71 ±0.08	0.56 ±0.07	0.37 ±0.05	0.90 ±0.09	0.44 ± 0.05	0.47 ±0.02	0.30 ±0.04	0.30 ±0.05	0.54 ±0.07
$log\tau_B$	-0.32 ±0.15	-0.64 ±0.07	n.a.	n.a.	n.a.	n.a.	n.a.	n.a.	n.a.	n.a.
	HEK293-$mGlu_5$ (high): assuming neutral affinity cooperativity (α=1)									
	CDPPB	VU29	CPPHA	VU0357121	VU0364289	VU0092273	VU0360172	VU0405398	VU0415051	VU0405386
pK_B	6.99±0.04	6.59 ±0.13	5.55 ±0.14	6.00 ±0.15	5.83 ±0.20	6.68 ±0.06	7.07 ±0.14	7.29 ±0.20	8.02 ±0.25	8.00 ±0.29
$log\beta$	0.29 ±0.05	0.54 ±0.13	0.58 ±0.07	0.92 ±0.01	0.78 ±0.05	0.77 ±0.11	0.88 ±0.15	0.87 ±0.06*	0.74 ±0.19	1.10 ±0.16*
$log\tau_B$	0.00 ±0.01	-0.05 ±0.06	-0.14 ±0.15	n.a.	-0.38 ±0.03	-0.23 ±0.04	-0.13 ±0.07	-0.69 ±0.15	-0.19 ±0.11	-0.14 ±0.03

Interactions between glutamate and allosteric modulators where quantified using equation 2 (where α=1), equation 3 (where τ_B=0) or equation 4 (where $\alpha\beta$ determined) where glutamate affinity was held constant to a previously reported value ($logK_A$ = -6.155; Mutel et al., 2000). The presence of allosteric modulators did not affect estimates of glutamate coupling efficiency ($log\tau_A$), the transduction coefficient (n), the maximal system response (E_m) and the basal level of response; the assumption that α=1, also had no effect on these estimates (one-way ANOVA, supplementary table 1). In the low-expressing cell line when $\alpha\beta$ was

determined: $\log\tau_A$= 0.75±0.03, n=2.54±0.12, E_m=102.5±1.0 and basal=1.0±0.17; when α=1: $\log\tau_A$= 0.80±0.02, n=2.66±0.13, E_m=103.5±1.07 and basal=1.15±0.19. In the high expressing cell line: $\log\tau_A$=0.37±0.02, n=2.84±0.16, E_m=118.3±2.3, basal= 0.81±0.23.

[a] negative logarithm of the allosteric modulator equilibrium dissociation constant.

[b] logarithm of the composite cooperativity factor, αβ, encompassing both affinity and efficacy modulation, quantified using equation 4.

[c] logarithm of the coupling efficiency of allosteric modulator.

[d] logarithm of the efficacy cooperativity factor, β, quantified using either equation 2 or 3 as appropriate.

n.a. denotes not applicable due to lack of appreciable agonism by allosteric modulator.

* significantly different to value for modulator determined in HEK293A-$mGlu_5$(low) for Ca^{2+} mobilization, $p<0.05$, one-way ANOVA, Tukey's post-test.

Table 3: Summary of operational model parameters for negative allosteric modulation of glu-mediated intracellular Ca^{2+} mobilization using HEK cells expressing low and high levels of $mGlu_5$. Data represent the mean and s.e.m from a minimum of three independent determinations.

	HEK293A-$mGlu_5$ (low): allowing for affinity modulation (α unconstrained)					
	MPEP	M-5MPEP	VU0285683	VU0366248	VU0366249	VU0366058
pK_B[a]	8.44 ±0.12	6.99 ±0.14	7.40 ±0.17	6.62 ±0.13	6.36 ±0.08	6.71 ±0.20
logβ[b]	-100[e]	-0.75 ±0.05	-100[e]	-0.83 ±0.10	-0.59 ±0.08	-100[e]
logα	0.12 ±0.06	0.25 ±0.07	0.20 ±0.11	-0.04 ±0.14	0.25 ±0.12	0.41 ±0.14
	HEK293A-$mGlu_5$ (low): assuming neutral affinity cooperativity (α=1)					
	MPEP	M-5MPEP	VU0285683	VU0366248	VU0366249	VU0366058
pK_B	8.55 ±0.09	7.04 ±0.15	7.59 ±0.10	6.63 ±0.08	6.35 ±0.08	7.09 ±0.10
logβ	-100[e]	-0.72 ±0.05	-100[e]	-0.90 ±0.09	-0.52 ±0.10	-100[e]
	HEK-$mGlu_5$ (high)					
	MPEP	M-5MPEP	VU0285683	VU0366248	VU0366249	VU0366058
pK_B	8.53 ±0.03	7.14 ±0.08	7.55 ±0.06	6.72 ±0.07	6.58 ±0.04	6.69 ±0.07
logβ	-100[e]	-100[e]	-100[e]	-100[e]	-0.48 ±0.04	-100[e]

Refer to footnotes of Table 2 for definitions of pK_B and logβ, as well as details on quantification. See supplementary Table 2 for estimates of glutamate coupling efficiency ($log\tau_A$), the transduction coefficient (n), the maximal system response (E_m) and the basal level of response.
[e] where a NAM abolished the response to glutamate it was assumed that β=0, thus logβ was constrained to -100.

Table 4: Summary of operational model parameters for allosteric modulation of glu-mediated ERK1/2 phosphorylation using HEK cells expressing a low level of $mGlu_5$. Data represent the mean and s.e.m from a minimum of three independent determinations.

	Positive allosteric modulators									
	CDPPB	VU29	CPPHA	VU0357121	VU0364289	VU0092273	VU0360172	VU0405398	VU0415051	VU0405386
pK_B	7.39 ±0.18	7.63 ±0.25*	6.88 ±0.14	7.56 ±0.30	6.29 ±0.11*	7.16 ±0.08	7.16 ±0.26	7.62 ±0.32	8.32 ±0.21	8.45 ±0.19
logβ	0.13 ±0.05	0.25 ±0.10	0.05 ±0.02	0.03 ±0.02	0.16 ±0.02	0.11 ± 0.02	0.12 ±0.04	0.05 ±0.05	0.03 ±0.02	0.19 ±0.07
$log\tau_B$	-0.05 ±0.11	-0.07 ±0.08	-0.13 ±0.05	-0.17 ±0.08	0.04 ±0.05	0.01 ±0.02	0.00 ±0.03	-0.39 ±0.20	-0.27 ±0.08	0.00 ±0.11

	Negative allosteric modulators					
	MPEP	M-5MPEP	VU0285683	VU0366248	VU0366249	VU0366058
pK_B	8.20 ±0.32	6.60 ±0.07	7.74 ±0.14	6.37 ±0.23	6.40 ±0.19	7.23 ±0.25
logβ	-100	-100	-100	-100	-0.31±0.12	-100

Refer to footnotes of Table 2 for parameter definitions.
For ERK1/2 phosphorylation in the low-expressing cell line, data were expressed as fold increase over basal, with the E_m defined as the response to 10% FBS (9.4 fold). In the presence of allosteric modulator, $log\tau_A$ (-0.36±0.13) and n (4.43±0.50) were not significantly different (one-way ANOVA; supplementary table 3).
* significantly different to value for modulator determined in HEK293A-mGlu5(low) for Ca^{++} mobilization, $p<0.05$, one-way ANOVA, Tukey's post-test.

Table 5: Quantification of impact of single point mutations on $mGlu_5$ allosteric modulator pharmacology. Data represent the mean and s.e.m from a minimum of three independent determinations.

	MPEP	VU29		CPPHA	
	pK_B	pK_B	logβ	pK_B	logβ
R5-wild type	8.58 ±0.17	6.87 ±0.19	0.40 ±0.03	5.62 ±0.16	0.78 ±0.14
R5-F585I	8.28 ±0.15	n.d.	n.d.	5.14 ±0.15	0.61 ±0.07
R5-Y658V	6.57±0.13*	n.d.	n.d.	n.d.	n.d.
R5-L743V	8.04 ±0.10*	6.52 ±0.17	1.04 ±0.09*	n.d.	n.d.
R5-A809V	6.52 ±0.12*	5.31 ±0.26*	0.58 ±0.10	n.d.	n.d.

Refer to footnotes of Table 2 for parameter definitions.
* indicates significantly different to wild type value, $p<0.05$, one-way ANOVA, Dunnett's post test.
n.d. indicates not determined.

Table 6: Estimates of allosteric modulator affinity from modulator concentration response curves in the presence of an EC_{20} (PAMs) or EC_{80} (NAMs) concentration of agonist. Data represent the mean and s.e.m from a minimum of three independent determinations.

	Modulator potency	Operational analysis of potency curves		From maximal fold shift
	PAM pEC_{50}[a]; NAM pIC_{50}[b]	pK_B[c]	$log\beta$[d]	$log\beta'$[e] (fold shift)
CDPPB	7.16 ±0.08	6.85 ±0.08	0.56 ±0.05	0.78 ±0.14 (7.1)
VU29	7.25 ±0.14	6.65 ±0.20	0.88 ±0.13	0.85 ±0.12 (8.8)
CPPHA	6.35 ±0.19	5.51 ±0.09	0.76 [e]	0.76 ±0.13 (7.8)
VU0357121	6.72 ±0.12	6.46 ±0.10	0.48 ±0.05	0.32 ±0.03 (2.1)
VU0364289	6.50 ±0.11	5.50 ±0.19	0.86 [e]	0.86 ±0.06 (7.6)
VU0092273[#]	7.05 ±0.08[#]	6.77 ±0.10	0.51 ±0.05	0.51 ±0.05 (3.3)
VU0360172[#]	7.45 ±0.07[#]	7.13 ±0.05	0.53 ±0.04	0.44 ±0.06 (2.8)
VU0405398	7.79 ±0.12	7.52 ±0.09	0.34 ±0.05	0.29 ±0.03 (2.0)
VU0415051	7.91 ±0.09	7.82 ±0.05	0.41 ±0.04	0.34 ±0.04 (2.3)
VU0405386	8.65 ±0.13	8.30 ±0.13	0.50 ±0.05	0.70 ±0.07 (5.3)
MPEP	8.07 ±0.07	8.10 ±0.17	-100[f]	n.a.
M-5MPEP	6.66 ±0.09	6.85 ±0.13	-0.41 ±0.03	n.a.
VU0285683	6.93 ±0.15	7.06 ±0.15	-100[f]	n.a.
VU0366248	5.85 ±0.13	6.24 ±0.13	-0.70 ±0.13	n.a.
VU0366249	5.74 ±0.20	5.73 ±0.19	-0.22 ±0.01	n.a.
VU0366058	6.52 ±0.27	6.64 ±0.11	-100[f]	n.a.

Operational analysis of potency curves was performed by simultaneously applying equations 6 and 7, where pK_A was constrained to 6.155, to derive pK_B and log β estimates for modulators.

[a] negative logarithm of the concentration of modulator that causes a half maximal potentiation of a low concentration (EC_{20}) of glutamate (equation 5).

[b] negative logarithm of the concentration of modulator that causes a half maximal inhibition of a sub maximal concentration (EC_{80}) of glutamate (equation 5).

[c] negative logarithm of the equilibrium dissociation constant of an allosteric modulator.

[d] logarithm of the efficacy cooperativity factor β.

[e] logarithm of the efficacy cooperativity factor β estimated from the maximal leftward shift of the glutamate curve caused by allosteric modulator, for PAMs that potentiated up to the maximal response of glutamate, logβ was constrained to this value to estimate affinity.

[f] where a NAM abolished the response to glutamate it was assumed that β=0, thus logβ was constrained to -100.

[#] potentiator concentration-response curves previously reported in Noetzel et al., 2011.

n.a. denotes not applicable.

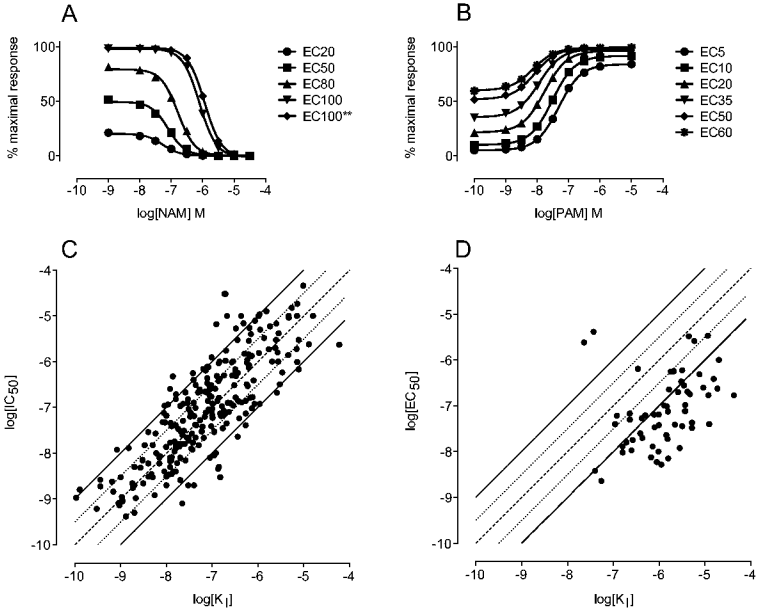
A
% maximal response
100
50
0
EC20
EC50
EC80
EC100
EC100**
-10 -9 -8 -7 -6 -5 -4
log[NAM] M
B
% maximal response
100
50
0
EC5
EC10
EC20
EC35
EC50
EC60
-10 -9 -8 -7 -6 -5 -4
log[PAM] M
C
log[IC50]
-4 -5 -6 -7 -8 -9 -10
-10 -9 -8 -7 -6 -5 -4
log[KI]
D
log[EC50]
-4 -5 -6 -7 -8 -9 -10
-10 -9 -8 -7 -6 -5 -4
log[KI]

Figure 1

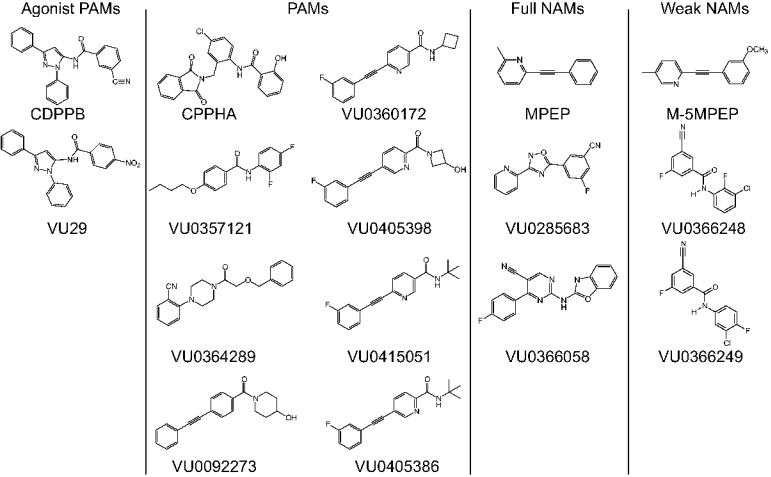
Agonist PAMs
PAMs
Full NAMs
Weak NAMs
CDPPB
CPPHA
VU0360172
MPEP
M-5MPEP
VU29
VU0357121
VU0405398
VU0285683
VU0366248
VU0364289
VU0415051
VU0366058
VU0366249
VU0092273
VU0405386

Figure 2

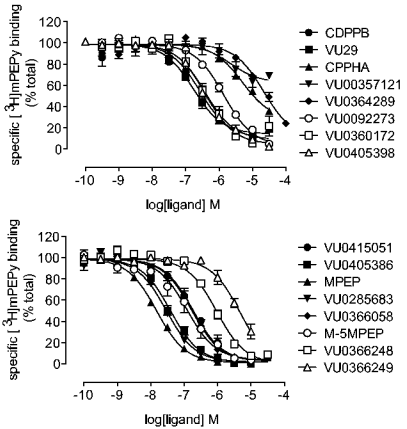
specific [3H]mPEPy binding (% total)
120
100
80
60
40
20
0
-10
-9
-8
-7
-6
-5
-4
log[ligand] M
CDPPB
VU29
CPPHA
VU00357121
VU0364289
VU0092273
VU0360172
VU0405398
specific [3H]mPEPy binding (% total)
120
100
80
60
40
20
0
-10
-9
-8
-7
-6
-5
-4
log[ligand] M
VU0415051
VU0405386
MPEP
VU0285683
VU0366058
M-5MPEP
VU0366248
VU0366249

Figure 3

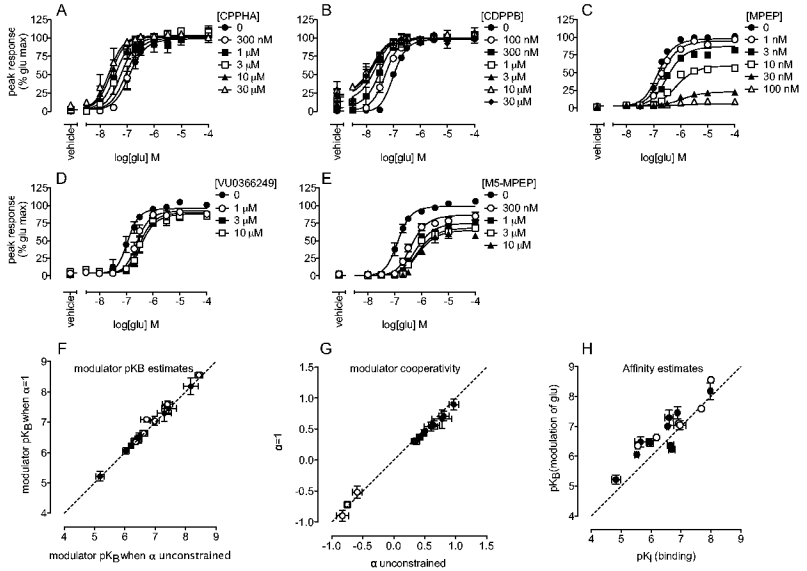
A
[CPPHA]
0
300 nM
1 μM
3 μM
10 μM
30 μM
peak response (% glu max)
log[glu] M
vehicle
B
[CDPPB]
0
100 nM
300 nM
1 μM
3 μM
10 μM
30 μM
C
[MPEP]
0
1 nM
3 nM
10 nM
30 nM
100 nM
D
[VU0366249]
0
1 μM
3 μM
10 μM
E
[M5-MPEP]
0
300 nM
1 μM
3 μM
10 μM
F
modulator pKB estimates
modulator pKB when α=1
modulator pKB when α unconstrained
G
modulator cooperativity
α=1
α unconstrained
H
Affinity estimates
pKB (modulation of glu)
pKI (binding)

Figure 4

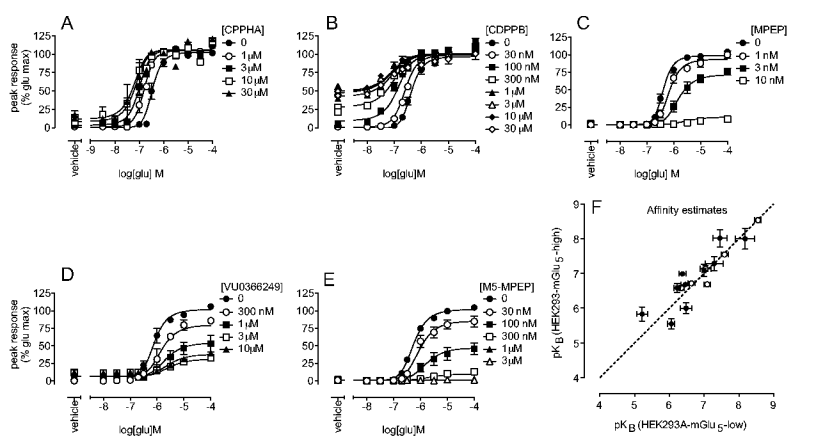
A
[CPPHA]
0
1 μM
3 μM
10 μM
30 μM
peak response (% glu max)
log[glu] M
vehicle
B
[CDPPB]
0
30 nM
100 nM
300 nM
1 μM
3 μM
10 μM
30 μM
log[glu]M
C
[MPEP]
0
1 nM
3 nM
10 nM
log[glu] M
D
[VU0366249]
0
300 nM
1 μM
3 μM
10μM
E
[M5-MPEP]
0
30 nM
100 nM
300 nM
1 μM
3 μM
F
Affinity estimates
pK B (HEK293-mGlu 5 -high)
pK B (HEK293A-mGlu 5 -low)

Figure 5

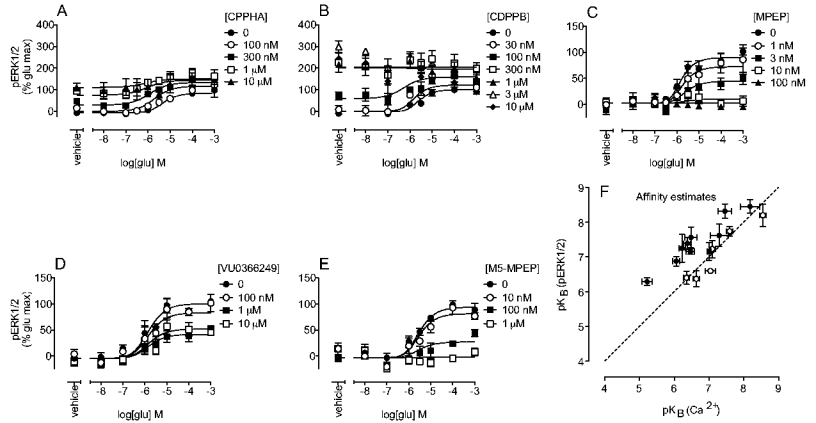
A
[CPPHA]
0
100 nM
300 nM
1 μM
10 μM
pERK1/2
(% glu max)
vehicle
log[glu] M
B
[CDPPB]
0
30 nM
100 nM
300 nM
1 μM
3 μM
10 μM
C
[MPEP]
0
1 nM
3 nM
10 nM
100 nM
D
[VU0366249]
0
100 nM
1 μM
10 μM
E
[M5-MPEP]
0
10 nM
100 nM
1 μM
F
Affinity estimates
pK B (pERK1/2)
pK B (Ca 2+)

Figure 6

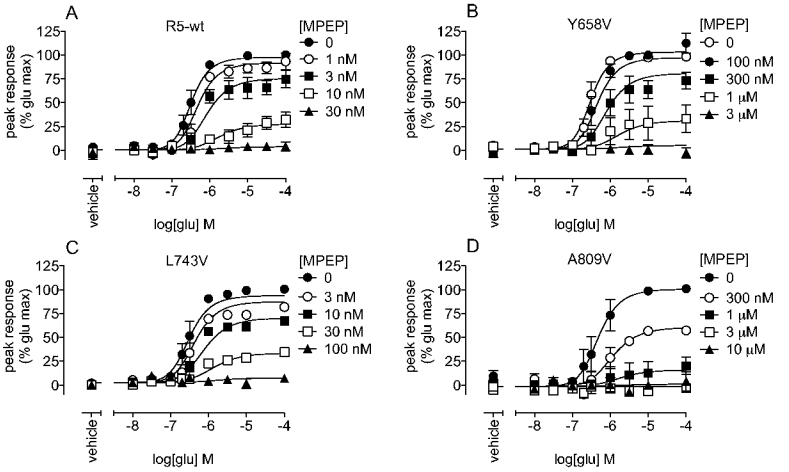
A
R5-wt
[MPEP]
0
1 nM
3 nM
10 nM
30 nM
peak response
(% glu max)
125
100
75
50
25
0
vehicle
-8
-7
-6
-5
-4
log[glu] M
B
Y658V
[MPEP]
0
100 nM
300 nM
1 μM
3 μM
C
L743V
[MPEP]
0
3 nM
10 nM
30 nM
100 nM
D
A809V
[MPEP]
0
300 nM
1 μM
3 μM
10 μM

Figure 7

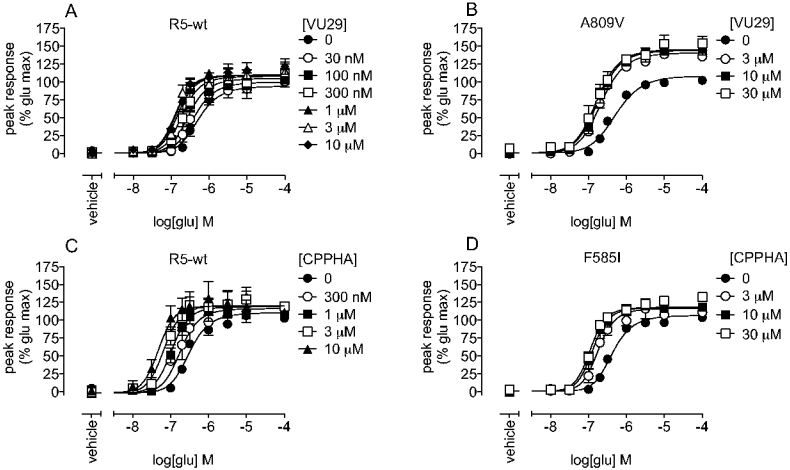
A
R5-wt
[VU29]
0
30 nM
100 nM
300 nM
1 μM
3 μM
10 μM
peak response
(% glu max)
175
150
125
100
75
50
25
0
vehicle
-8
-7
-6
-5
-4
log[glu] M
B
A809V
[VU29]
0
3 μM
10 μM
30 μM
C
R5-wt
[CPPHA]
0
300 nM
1 μM
3 μM
10 μM
D
F585I
[CPPHA]
0
3 μM
10 μM
30 μM

Figure 8

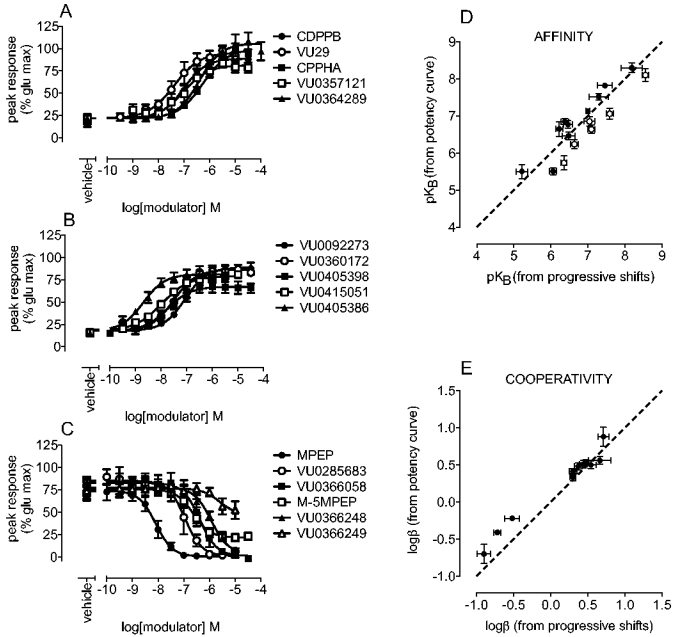
A
peak response (% glu max)
CDPPB
VU29
CPPHA
VU0357121
VU0364289
vehicle
log[modulator] M
B
VU0092273
VU0360172
VU0405398
VU0415051
VU0405386
C
MPEP
VU0285683
VU0366058
M-5MPEP
VU0366248
VU0366249
D
AFFINITY
pKB (from potency curve)
pKB (from progressive shifts)
E
COOPERATIVITY
logβ (from potency curve)
logβ (from progressive shifts)

Figure 9